REPORT DOCUMENTATION PAGE

Form Approved
OMB No. 0704-0188

1. REPORT DATE *(DD-MM-YYYY)*: 01062006

2. REPORT TYPE: Final Report

3. DATES COVERED *(From - To)*: 15 Jan 2003 - 31 Dec 2005

4. TITLE AND SUBTITLE

Ram Load Simulation of Wing Skin-Spar Joints: New Rate-Dependent Cohesive Model

5a. CONTRACT NUMBER

5b. GRANT NUMBER

F49620-03-C-0014

5c. PROGRAM ELEMENT NUMBER

5d. PROJECT NUMBER

5e. TASK NUMBER

5f. WORK UNIT NUMBER

6. AUTHOR(S)

Monty A. Moshier

7. PERFORMING ORGANIZATION NAME(S) AND ADDRESS(ES)

RHAMM Technologies LLC
332 Skyland Drive
Bellbrook OH 45305

8. PERFORMING ORGANIZATION REPORT NUMBER

9. SPONSORING/MONITORING AGENCY NAME(S) AND ADDRESS(ES)

USAF/AFRL
AFOSR
875 North Randolph Street
Arlington VA 22203

10. SPONSOR/MONITOR'S ACRONYM(S)

AFOSR

11. SPONSOR/MONITOR'S REPORT NUMBER(S)

12. DISTRIBUTION/AVAILABILITY STATEMENT

Distribution Statement A. Approved for public release; distribution is unlimiited.

Dr John Schmisseur

AFRL-SR-AR-TR-06-0104

13. SUPPLEMENTARY NOTES

14. ABSTRACT

A new rate-dependent cohesive zone model for use in impact and/or hydrodynamic ram delamination problems is presented. The traction based model includes a damage-dependent term and two cohesive zone viscosity parameters. The first viscosity parameter adjusts the yield traction of the material, while the second parameter adjusts the peak or maximum traction. This new rate-dependent cohesive model is implemented in LS-DYNA (971 beta revision 5397), an explicit time integration FEA code, by defining a user cohesive material model. It may be used with shell or brick elements. Previously published Double cantilever beam (DCB) experiments of epoxy and PEEK/carbon-fiber composites are modeled in order to validate the rate-dependent cohesive model. Also, in order to provide a methodology to obtain data to determine material constants for this rate-dependent cohesive zone model, a simple inexpensive experimental apparatus for high rate DCB (Double Cantilever Beam) sample testing was developed.

15. SUBJECT TERMS

16. SECURITY CLASSIFICATION OF: a. REPORT	b. ABSTRACT	c. THIS PAGE	17. LIMITATION OF ABSTRACT	18. NUMBER OF PAGES	19a. NAME OF RESPONSIBLE PERSON / 19b. TELEPHONE NUMBER *(Include area code)*
U	U	U	UU	78	

Report Number: RHAMM-TR-05-01
January 6, 2006

Ram Load Simulation of Wing Skin-Spar Joints: New Rate-dependent Cohesive Model

Brian. D. Choules, Monty A. Moshier and Ronald L. Hinrichsen

RHAMM Technologies LLC
332 Skyland Dr., Bellbrook
OH 45305

Prepared for
United States Air Force
under Contract No. F49620-03-C-0014

UNCLASSIFIED

This material is based upon work supported by the United States Air Force under Contract No. F49620-03-C-0013.Any opinions, findings and conclusions or recommendations expressed in this material are those of the author(s) and do not necessarily reflect the views of the United States Air Force.

Abstract

A new rate-dependent cohesive zone model for use in impact and/or hydrodynamic ram delamination problems is presented. The traction based model includes a damage-dependent term and two cohesive zone viscosity parameters. The first viscosity parameter adjusts the yield traction of the material, while the second parameter adjusts the peak or maximum traction. This new rate-dependent cohesive model is implemented in LS-DYNA (971 beta revision 5397), an explicit time integration FEA code, by defining a user cohesive material model. It may be used with shell or brick elements. Previously published Double cantilever beam (DCB) experiments of epoxy and PEEK/carbon-fiber composites are modeled in order to validate the rate-dependent cohesive model. Also, in order to provide a methodology to obtain data to determine material constants for this rate-dependent cohesive zone model, a simple inexpensive experimental apparatus for high rate DCB (Double Cantilever Beam) sample testing was developed.

Table of Contents

Figures

Tables

Preface

A new rate-dependent model for fracture of composite materials is presented. Additionally, an inexpensive experimental apparatus is presented which provides the data necessary for the rate-dependent model. Code is presented which can be used as a user material with the finite element explicit package LS-DYNA (971 beta revision 5397). This new rate-dependent model can be used with any application where rate-dependent failure is important. Specifically, the model is applied to survivability of composite material under hydrodynamic ram. The model presented includes only mode I rate-dependence and may be used with shell and solid elements.

The authors thank the Aerospace Survivability and Safety Flight of the 46th Test Wing at Wright Patterson Air Force Base for continued support and use of test facilities.

1 Summary

A new rate-dependent cohesive zone model for use in impact mode I delamination problems is presented. The traction based model includes a damage-dependent term and two cohesive zone viscosity parameters. The first viscosity parameter adjusts the yield traction of the material, while the second parameter adjusts the peak or maximum traction. LS-DYNA (971 beta revision 5397), an explicit time integration FEA code, is used to model double cantilever beam (DCB) experiments of fiber composites with loading rates varied from 0.65 m/s to 20 m/s. The rate-dependent cohesive zone model is used to formulate a rate-dependent cohesive element for use with shell or solid elements. This rate-dependent cohesive model is implemented in LS-DYNA by defining a user cohesive material model. Using previously published data, epoxy and PEEK/carbon-fiber composites are found to require a rate-dependent cohesive model to adequately model the experiments. The rate-dependent cohesive zone model presented, with a single set of constants for each material, produces agreement between the experimental and FEA results.

A simple inexpensive experimental apparatus for high rate DCB (Double Cantilever Beam) sample testing was developed. The apparatus uses a cocked spring mechanism to provide high rate mode I loading to a pre-cracked DCB specimen. Testing of six samples was performed. Loading rates varying from 0.6 to 14.5 m/s were obtained. A finite element analysis simulating the testing of DCB samples was performed. Comparisons with the rate-independent ($\nu=\eta=0$) and rate-dependent ($\eta\neq0$) cohesive model and the experimental data were performed. It was determined that the rate-dependent model provided better agreement with the experimental data than the rate-independent model.

2 Introduction

2.1 Background

The use of polymer matrix composites and bonded and/or co-cured assemblies in airframe structures has shown promise in achieving the performance and cost goals of next generation fighter/attack aircraft. The weight and/or affordability benefits may be limited, however, by the need to meet survivability requirements. The current survivable design procedure is to size a structure for flight, fuel pressure, crash, etc. loads and then ballistically test the resulting design to determine its survivability capability. For metal structures, this remains a feasible process since there are plenty of historical ballistic test data available for use in developing design requirements. However, this is not the case for composite structures.

The typical manned fighter survivability design goal, defined by the Live Fire Law[1], of 55% design limit load (DLL) residual strength after damage from a 30mm high explosive incendiary (HEI) threat has not yet been demonstrated on an all-composite platform. (Unmanned vehicles and non-fighter aircraft will have less stringent requirements.) In attempting to meet the Live Fire Law requirements, the F-22 program conducted several ballistic tests on all-composite wing designs without success. Ballistic tolerance was finally accomplished by replacing five bolted composite spars with five bolted titanium spars. This cost the program thousands of dollars per aircraft and schedule slippage and development costs as well as additional weight in each aircraft.

The Air Force and Navy consider the survivability problem of an all-composite structure critical and have invested a significant amount of funding to address this issue. The Air Force's Decoupled Fuel Cells (DFC) program [2] identified the benefits of addressing survivability earlier in the design phase with cost and weight savings using a cocured wing design for the F-22 and eliminating the titanium spars. This study demonstrated that a wing design that relies on a bolted metal substructure to meet the live fire requirements for combat aircraft can cost and weigh substantially more than a survivable composite design. Furthermore, the promise of future weight and cost savings can only be realized by addressing the survivability of composite structures early in the design phase of an aircraft.

Advanced processing techniques, interlaminar reinforcement technologies and innovative design concepts have been developed in recent years and provide significant improvements towards achieving a survivable, all-composite wing structure while minimizing its weight and cost. Until the execution of the Composites Affordability Initiative (CAI) in the late 1990's, industry lacked a set of rules and procedures that could guide engineers in incorporating these survivability features early in the structural design process. The Survivability Group of the CAI Pervasive Team drafted the HRAM Survivability Design Guidelines [3], which contained this direction so that the weight and cost goals could be met. The use of these guidelines will reduce the design and analysis development time by greatly minimizing the need for redesigns after the ballistic testing is completed. Their use will also potentially reduce the amount of costly testing needed by providing a history of ballistic test results and proven designs for damage containment. Ballistic testing cannot be completely eliminated from the process, but the cost of testing can be reduced by testing smaller articles and incorporating historical test data into the design process.

The general sequence for designing for survivability (as specified in the Design Guidelines) is as follows:

1) Develop/Identify the survivability requirements for the program ,
2) Design the structure for flight and hydrodynamic ram (HRAM) loads, conduct developmental testing, and
3) Ballistically test the final designs, either full-scale articles or large subcomponents.

Implied within 2) above is the assumption that the designer has validated and reliable modeling and simulation (M&S) tools at his disposal in order to perform analyses which will assist him in converging on an optimum design. Although the Survivability Group of the CAI Pervasive Team made significant progress in this area, they identified two shortcomings specifically with the hydrodynamic ram analysis techniques, which must be resolved before the tools can be declared robust. These shortcomings are:

1) More work is needed to accurately model the details that differentiate one joint design from another. The incorporation of stitching, z-pinning, co-curing, and bonding of the joints leads to different failure modes and paths. The area in which most work is needed is in the proper selection of failure criteria within the joints as well as the entire model. Right now, the state-of-the-art is to use the elastic-plastic smeared properties technique in modeling the structure and "fuze elements" to model the joints.

2) High loading rates encountered in hydrodynamic ram (HRAM) events are neither well understood nor well characterized. As rate dependent material properties are determined and documented, the analysis codes must have the capability to incorporate them. Although there is limited capability in this regard, more work is needed.

These issues are significant in accurately predicting the survivability of multi-sparred, fuel-filled composite wing structures. The plan for such wings is to have enough structural integrity remaining after impact to carry the loads. If the design tools aren't accurate, they may over or under predict the viability of the remaining structure. In either case, increased cost (in terms of dollars, time, and human life) may ultimately result.

Historically, the failure of joints is the result of fast fracture that occurs in resin rich zones of the composite joints. The development and implementation of fracture mechanics concepts into explicit time integration FEA coding is required if such events are to be modeled. Additionally, the development of a fracture mechanics based model for energy release rate as a function of the crack opening rate is needed to account for the high loading rates caused by HRAM.

2.2 Project Objectives

There were three main objectives of the proposed work:

1) Develop a fracture mechanics based model for energy release rate as a function of crack opening displacement (COD) rate in co-cured and bonded organic composites.

   a) Conduct basic research into improving the current stress/strain failure criteria which are not robust enough to model high loading rate fracture failure.

   b) Develop a basic method for acquiring energy release rate data that is high loading rate dependent. A simple double cantilever beam (DCB) specimen will be used for the data collection.

   c) Use the data from 1.b in order to develop an empirical based model relating COD rate to energy release rate. Using fracture mechanics concepts a release pressure (traction-separation law) will then be derived.

2) Develop a finite element formulation for incorporating into an explicit time integration finite element analysis package a nodal/element based method for describing a force/stress based fracture.

   a) Incorporate the best practices found in their basic research of 1a. through 1c. into a finite element formulation.

   b) Demonstrate through modeling and simulation of a simple DCB specimen the applicability of the new high loading rate failure mechanism.

3) Validate the new finite element formulation and high COD rate fracture mechanics based failure mechanism.

   a) RHAMM Technologies, LLC will complete validation by comparing the DCB modeling results with DCB experimental high strain rate data.

   b) RHAMM Technologies, LLC will build a finite element model of simple composite wing box and demonstrate joint failure using the new failure mechanism under HRAM loading.

All objectives with exception of 3b were met. The personnel involved in this work are presented in Appendix A1. The publications resulting from this work are presented in Appendix A2.

2.3 Statement of scope

All Live Fire Testing and Evaluation (LFT&E) and Joint Live Fire (JLF) and other vulnerability assessments are negatively impacted by the lack of analysis capability. This is particularly crucial to the design of new aircraft, such as the Joint Strike Fighter (JSF), which have multiple live fire requirements. Because the JSF and future aircraft will use significantly more composites than their predecessors, new design tools are needed. Without a complete analysis capability that includes the ability to model composite joint concepts, designers are forced to build and test composite boxes that are extremely expensive. When fully developed, this concept will provide tools for accurately predicting the survivability of multi-sparred, fuel-filled composite wing structures.

2.4 Report Organization

The experimental apparatus for testing DCB samples at high strain rates is presented in Section 3.1. The new rate-dependent cohesive model is presented in Section 3.2, while the details of the LS-DYNA FEA model are presented in Section 3.3. The validation of the rate-dependent cohesive element developed in this research is presented in Section 4.1. This validation compares experimental data at various rates of composite DCB samples from literature to the FEA results using cohesive model with and without rate-dependence. Section 4.2 presents the experimental data obtained using the high rate DCB testing apparatus developed during this study. Finally in Section 4.3, the cohesive model is used to model these experiments and the results are compared to the experimental data. Conclusions are presented in Section 5.

3 Methods, Assumptions and Procedures

3.1 High Strain Rate Experimental Apparatus

An experimental apparatus that may be used to test DCB test articles at high loading/strain rates was designed, built and tested. This section describes the DCB specimens testing, the experimental apparatus design, and the experimental results.

3.1.1 DCB Experimental Specimen

A schematic drawing and photograph of the DCB experimental specimen are shown in Fig. 1. The specimens are 25.4 mm wide, 229 mm long, and 3.05 mm thick, with an initial crack of 25.4 mm at one end, artificially simulated by a Teflon separator 25.4 mm wide and 0.025 mm thick, inserted in the mid-surface of the laminate. T-shaped aluminum tabs (12.7 mm wide, 25.4 mm long, and 3.18 mm thick) are attached to the DCB specimens using a two part epoxy adhesive. White reference dots were painted on the side of each DCB specimen to facilitate crack velocity and deflection measurements.

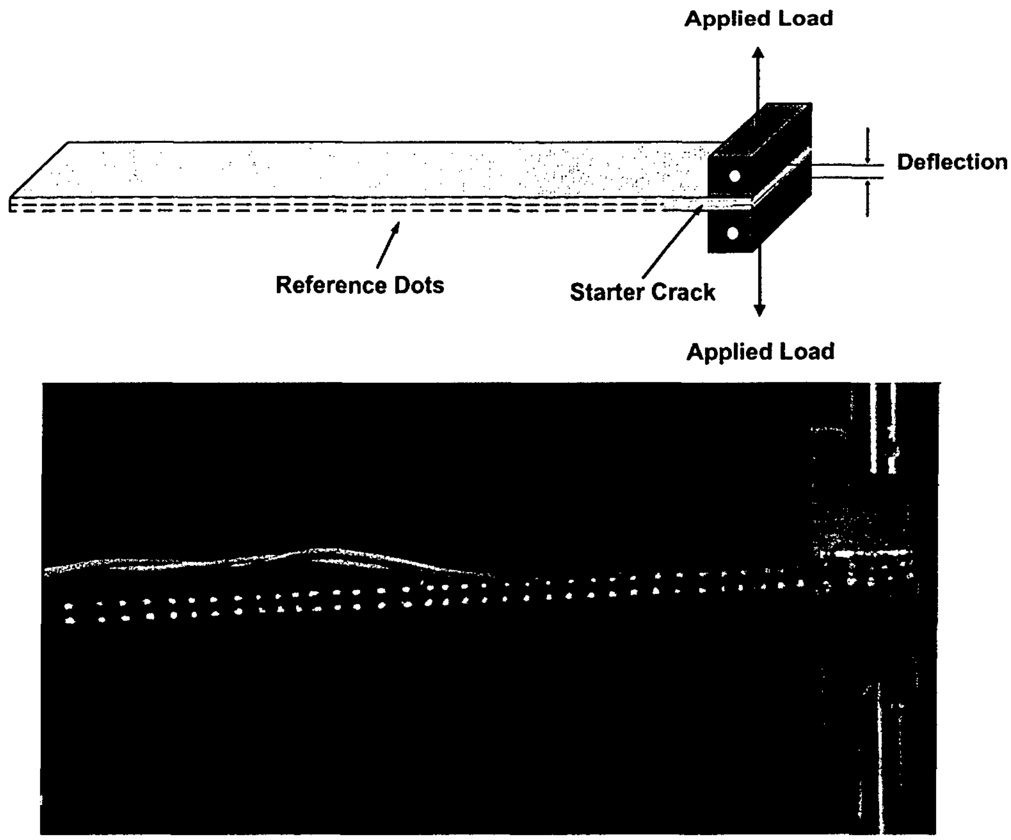

Figure 1. DCB experimental specimen setup and loading: schematic and photograph.

3.1.2 DCB Experimental Apparatus

The experimental testing setup includes a high rate loading test machine, high speed digital video camera (Phantom V7), TEMA (TrackEye Motion Analysis) software, and LabView data acquisition system for collecting strain and load data. The drawings of this apparatus are contained in Appendix A3.

The high rate loading test machine was designed to store energy in a compression spring and quickly release the energy to load a double cantilever beam specimen. A cable is attached to each tab on the DCB. Each cable provides the loading as shown in Fig. 2. One end of the cable is fixed (load cell end) and one end is connected to a cable with an aluminum ball attached to the other end. The aluminum ball rests on a compression spring which is compressed and held with a lever until a trigger is pulled. When the trigger is pulled, the spring accelerates the aluminum ball pulling on the cable and pulling apart the DCB. Fig. 2 shows a sketch of the configuration at time t=0 and some time t>0 after the trigger has been pulled. Cocking the spring was accomplished by using a hand actuated hydraulic actuator to pull up on the cable attached to the compression spring before the specimen is loaded into the apparatus.

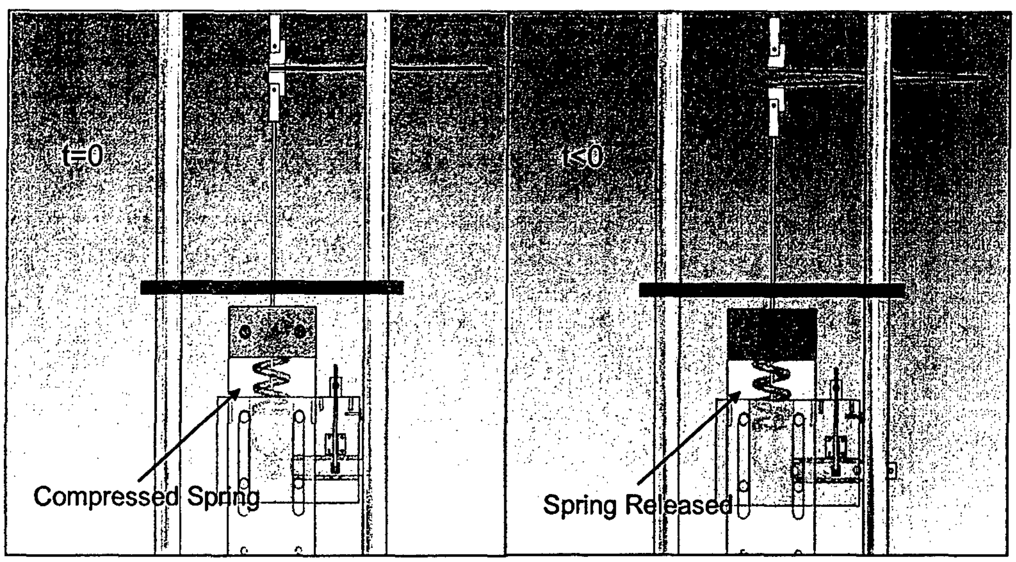

Figure 2. DCB test machine at t=0 and t>0

3.1.3 Data Collection and Analysis

A piezoelectric dynamic load cell is used to determine the applied load on the fixed end. Deflection at the applied load and crack velocity is measured from high speed digital video using TEMA software and white reference dots on the side of the DCB specimen. The Phantom V7 digital camera is set to collect *4800* frames per second at 800x600 pixels resolution. The digital video along with the TEMA software package provides the necessary capability to extract both crack tip velocity and crack opening displacement (COD).

3.2 Rate Dependent Cohesive Model Formulation

Cohesive models have been widely used to model dynamic crack growth (Chowdhury and R. Narasimhan 2000; Rahul-Kumar et al. 2000; Ruiz et al. 2001; La Saponara et al. 2002). Many models have been introduced including: extrinsic, intrinsic, perfectly plastic, linear softening, progressive softening, and regressive softening (Camanho and Dávila 2004). Several rate-dependent models have also been introduced (Glennie 1971; Xu et al. 1991; Costanzo and Walton 1997; Tvergaard and Hutchinson 1996; Fager and Bassani 1991; Kubair and Geubelle 2003). A rate-dependent cohesive zone model was first introduced by Glennie (1971) $\tau = \tau^{l}(1+\eta\dot{u})$, where the traction in the cohesive zone is a function of the crack opening displacement time derivative. Xu et al. (1991) extended this model by adding a linearly decaying damage law $\tau = \tau^{c}(1-u/u_{cr})(1+\eta\,\dot{u}/c_{s})$. In each model the viscosity parameter (η) is used to vary the degree of rate dependence. Kubair et al. (2003) thoroughly summarized the evolution of these rate-dependant models and provided the solution to the mode III steady–state crack growth problem as well as spontaneous propagation conditions.

The rate-dependent cohesive zone model resulting from this research is presented in Eq. (1-2). This model is unique it contains a rate-dependent term for the onset of the opening ($v\dot{u}$) of the cohesive zone combined with a maximum traction rate-dependent term ($\dot{u}\eta$). The model is also unique in that a cohesive zone starting or yielding displacement (u_s) may be defined to greatly increase numerical stability.The critical strain energy release rate, found by integrating over the appropriate crack opening displacements, is given by Eq. (3).

$$\tau = \begin{Bmatrix} (\tau_y + v\dot{u})\dfrac{u}{u_s} & \text{for } u \le u_s, \\ \tau_y + v\dot{u}_s + (\dfrac{\tau_{\max} + \dot{u}\eta - (\tau_y + v\dot{u}_s)}{u_{cr} - u_s})(u - u_s) & \text{for } u_s < u \le u_{cr}, \\ \dfrac{\psi(\tau_{\max} + \dot{u}_{cr}\eta)}{u_{cr}} u & \text{for } u_{cr} \le u \le u_{end}. \end{Bmatrix} \tag{1}$$

$$\begin{aligned} &\psi = 1 && \text{for } u \le u_{cr}, \\ &\psi = a - b\frac{1}{u} && \text{for } u_{cr} \le u \le u_{end}, \\ &\text{where} \\ &a = \frac{u_{cr}}{u_{cr} - u_{end}}, \\ &b = \frac{u_{end}u_{cr}}{u_{cr} - u_{end}}. \end{aligned} \tag{2}$$

$$
G_{Ic} = \left\{ \begin{array}{ll}
\int_0^{u_s} \tau_y \frac{u}{u_s} du + \int_{u_s}^{u_{cr}} \tau_y + (\frac{\tau_{\max} - \tau_y}{u_{cr} - u_s})(u - u_s) du + & \\
\int_{u_{cr}}^{u_{end}} \frac{\psi \tau_{\max}}{u_{cr}} u \, du, & \text{for } \eta = \nu = 0, \\
\int_0^{u_s} (\tau_y + \nu \dot{u}) \frac{u}{u_s} du + & \\
\int_{u_s}^{u_{cr}} \tau_y + \nu \dot{u}_s + (\frac{\tau_{\max} + \dot{u}\eta - (\tau_y + \nu \dot{u}_s)}{u_{cr} - u_s})(u - u_s) du + & \\
\int_{u_{cr}}^{u_{end}} \frac{\psi(\tau_{\max} + \dot{u}_{cr}\eta)}{u_{cr}} u \, du, & \text{for } \quad \eta \neq 0, \nu \neq 0.
\end{array} \right\} \tag{3}
$$

For mode II and III loading the cohesive model is rate-independent as presented in equations (4-6). The mode II and III crack opening displacements are combined according to equation (4) in order to form the damage constant ψ_{23}. The cohesive tractions are assigned with equations (5 and 6). This is a simple bi-linear model. The constant K_{23} is used for both mode II and III loadings for the hardening portion of the traction-separation curve, however two separate constants could easily be defined if needed. A rate-dependent model for mode II and III is left to another research work.

$$
u_{23} = \sqrt{u_{II}^{\ 2} + u_{III}^{\ 2}} \tag{4}
$$

$$
\tau_{II} = K_{23} u_{II} \psi_{23} \tag{5}
$$

$$
\tau_{III} = K_{23} u_{III} \psi_{23} \tag{6}
$$

$$
\psi_{23} = \left\{ \begin{array}{ll}
1 & \text{for } u_{23} \leq u_{23cr} \\
a_{23} - b_{23} \frac{1}{u_{23}} & \text{for } u_{23} \leq u_{23} \leq u_{23end}
\end{array} \right\}
$$

where

$$
a_{23} = \frac{u_{23cr}}{u_{23cr} - u_{23end}}, \qquad
b_{23} = \frac{u_{23end} u_{23cr}}{u_{23cr} - u_{23end}}. \tag{6}
$$

An example traction separation curve for the mode I rate-dependent portion of the model is shown in Figure 3. The initial portion of the traction separation curve is defined by two parameters: the yield stress τ_y and the displacement u_s. Typically, when the traction exceeds τ_y, this signals the nucleation of the cohesive zone. However, the author's found it necessary for u_s to be greater than zero but small (in this case, 0.001 μm) in order to facilitate numerical stability in the time explicit finite element numerical methodology. In the case of finding an analytical solution of a problem employing this cohesive model, the value of u_s may be set to zero.

The traction $\tau_{\max}$ is the maximum traction that can occur if no rate dependence ($\nu=\eta=0$) is present. This traction occurs at the critical displacement u_{cr}. For crack opening values larger than u_{cr}, the traction reduces linearly to zero at the crack opening of u_{end}. This occurs through the damage parameter ψ varies from one (at $u=u_{cr}$) to zero (at $u=u_{end}$). Through the viscosity term ν, rate-dependence is given to the yield traction τ_y, while the viscosity term η gives rate dependence to $\tau_{\max}$. The traction separation curve remains linear between u_s and u_{cr}, and between u_{cr} and u_{end} regardless of the values of ν and η. Figure 4 presents an example of a traction separation curve for an arbitrarily chosen displacement function $u(t)=500t^3$. For this example η is fixed ($\eta=0$) and ν is varied. As the cohesive zone viscosity increases, the critical strain energy release rate (G_c), represented by the area of the traction separation curve, increases linearly (see Figure 5). Figures 6 and 7 present the effect of varying the viscosity parameter η (with $\nu=0$) on the traction and critical strain energy release rate, respectively. Figure 8 shows the effect of varying both ν and η with $\eta=2\nu$. It should be noted that negative values of ν and η are permissible with the criteria that $\tau \geq 0$. Thus, when η is less zero and $\dot{u}$ is great enough to cause $\tau_{\max}$ to decrease to zero or below, the traction would necessarily be set to zero.

This model implemented in LS-DYNA as a cohesive user defined material property. The code contained in the file dyna21.f is presented in Appendix A4. The cohesive element in LS-DYNA is currently only available in a beta version of LS-DYNA (971 beta revision 5397)

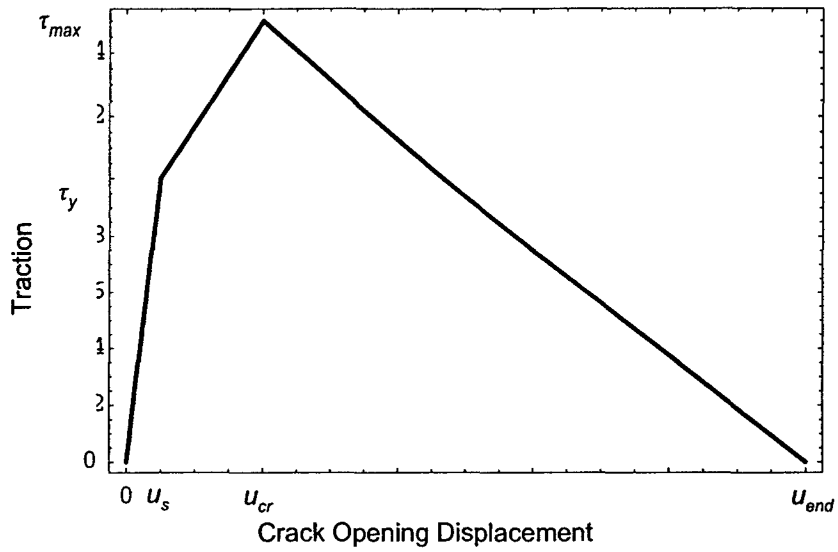

Figure 3. Example cohesive traction separation curve.

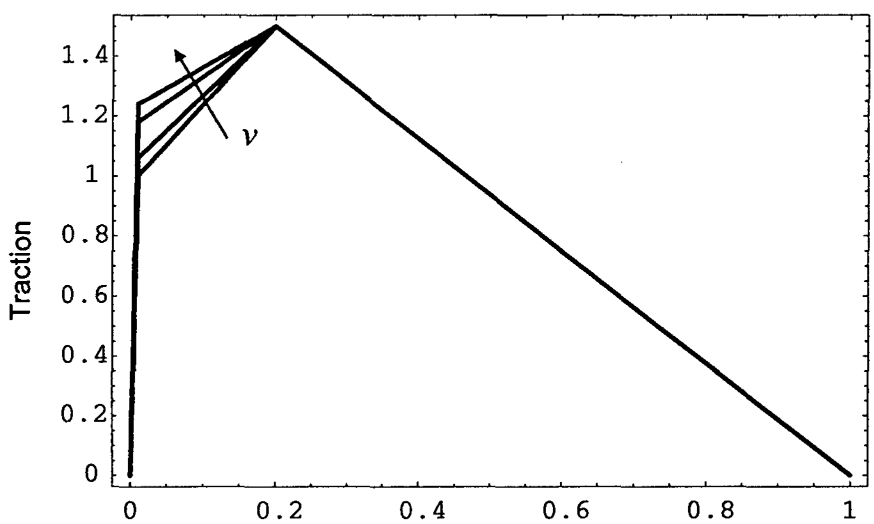

Figure 4. Cohesive traction separation curves, example for arbitrarily chosen *u(t)* with varied ν (with η=0).

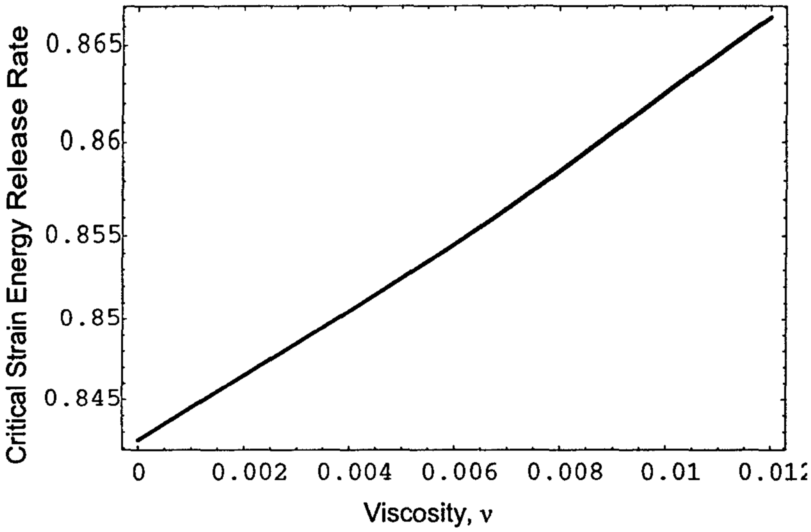

Figure 5. Critical strain energy release rate versus ν, example for arbitrarily chosen $u(t)$ with varied ν (with η=0).

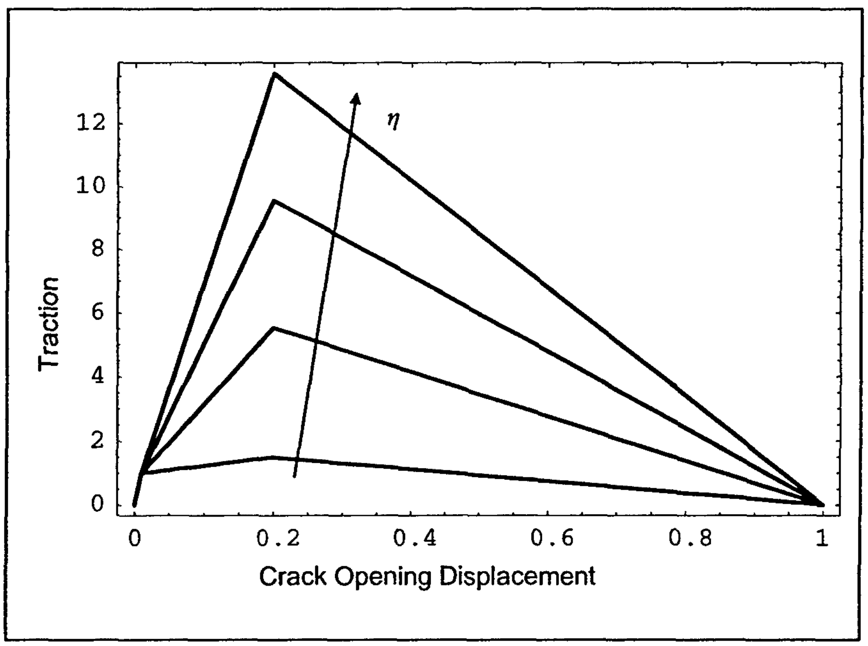

Figure 6. Cohesive traction separation curves, example for arbitrarily chosen $u(t)$ with varied η (with ν =0).

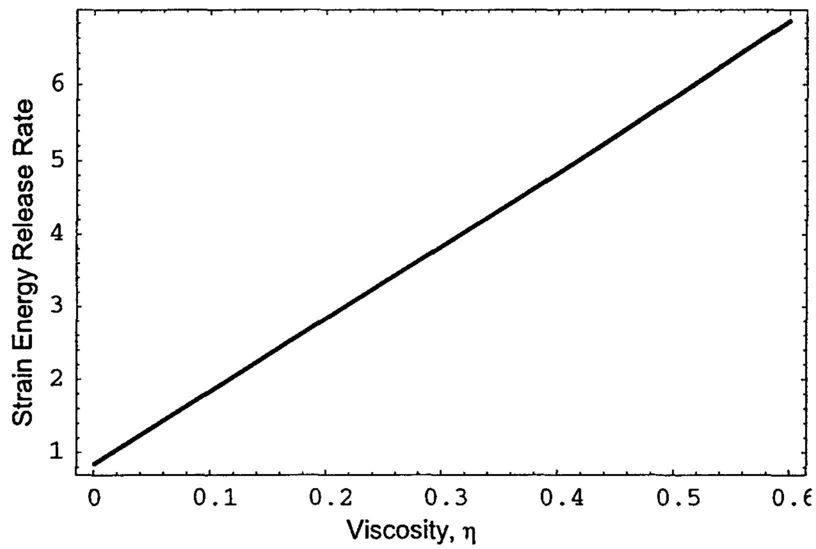

Figure 7. Critical strain energy release rate versus η, example for arbitrarily chosen *u(t)* with varied η (with ν =0).

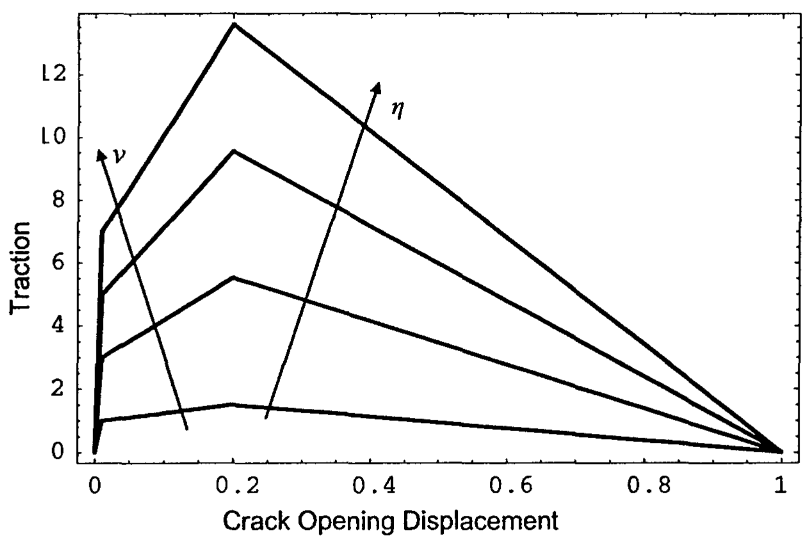

Figure 8. Cohesive traction separation curves, example for arbitrarily chosen *u(t)* with varied ν and η (with ν =2 η).

3.3 LS-DYNA FEA Modeling

The DCB specimen geometry modeled in this study is presented in Figure 9. The DCB specimen was modeled with 12500 shell elements, 13052 nodes, and 5500 cohesive elements. The specimen or shell element thickness (h_1 and h_2) of each arm of the DCB specimen was set to 1.5 mm. An initial crack length of approximately 30 mm was used, depending on the values evident from the reported data. The reported velocity was prescribed on the upper arm at a location 5 mm from the pre-cracked end of the specimen. The displacement of the bottom arm was fixed, while allowing free rotation at the same location. The material properties obtained by Blackman et al. (1995) were used. For the PEEK composite material, the bending modulus, density, and Poisson's ratio were 120 GPa, 1540 Kg/m^3, and 0.28, respectively. For the epoxy composite material, the bending modulus, density, and Poisson's ratio were 115 GPa, 1566 Kg/m^3, and 0.27, respectively. The effective bending modulus was found using a 3-point bend test (Blackman et al. 1995). The bending modulus was found to be rate-independent using an ultrasonic test rig utilizing Lamb waves. The critical portions of the LS-DYNA input (.key) files are included in appendix A5.

The crack length history data for each analysis are obtained by first running LS-Post. In LS-Post a line of nodes running in the direction of crack growth are selected on each cross section (upper and lower). The displacements in the direction of interest are then saved to a text file. The crack history extraction program given appendix A6 is then run. The user is prompted for filename where the displacement data is contained, the initial crack length, and the filename that contains the node XYZ coordinates.

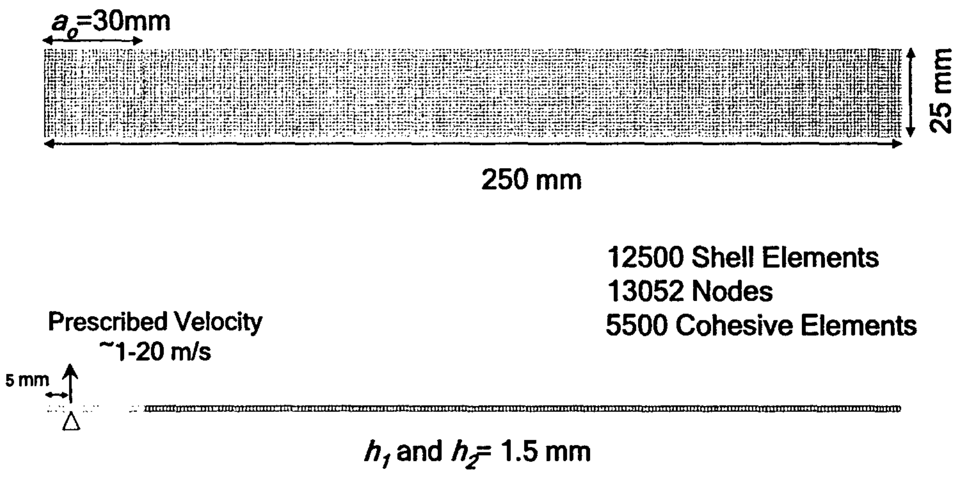

Figure 9. Finite element model of Blackman et al. (1995; 1996) DCB sample.

4 Results and Discussion

4.1 Rate Dependent Cohesive Model Results Validation

The rate-dependent cohesive zone model (section 3.2) was implemented using a user defined cohesive material model in LS-DYNA, an explicit time integration FEA code. The experiments performed by Blackman et al. (1995; 1996) were modeled. Two materials were analyzed PEEK/carbon-fiber and Epoxy/carbon-fiber composites at the testing rates reported by Blackman et al. (1995; 1996) varing from 0.65 m/s to 20.5 m/s. The specimen geometry and boundary conditions used in the FEA model are presented in Section 3.3, while the rate-independent ($\nu = \eta = 0$) and rate-dependent FEA results are presented in Sections 4.3.1 and 4.3.2, respectively.

4.1.1 FEA Rate-Independent Results

The crack length (a) versus time curves reported by Blackman et al. were compared to the rate-independent ($\nu=\eta=0$) cohesive zone FEA results for the appropriate loading rates. The critical strain energy release rate (G_c), according to Eq. (3), was set so that agreement between the experimental and finite element analysis crack length (a) versus time curves was obtained. Example crack length versus time plots for the PEEK and epoxy composite materials are presented in Figs. 10-13; showing a comparison of the rate-independent FEA results and the experimental results. Excellent agreement was found between the rate-independent and experimental results; however adjustment of the G_c was required for each rate in order to reach this agreement. Blackman et al. observed unstable "stick-slip" crack growth of the PEEK composite at a rate of 1.1 m/s. The rate-independent model ($\nu=\eta=0$) was not able to capture this behavior. G_c tended to increase with increasing loading rate for the epoxy composite material as shown in Fig. 14, however for the peek composite material G_c decreased with loading rate. In Fig. 14, the values of G_c obtained for this study are compared with those reported by Blackman et al. (1995). Reasonable agreement was found considering lack of complete information regarding the testing methodology. Table 1 presents the tabulated G_c values required for each case. From these results it may be concluded that a rate-dependent cohesive zone model is required to adequately model these materials and experimental results when significant variation in loading rate is expected.

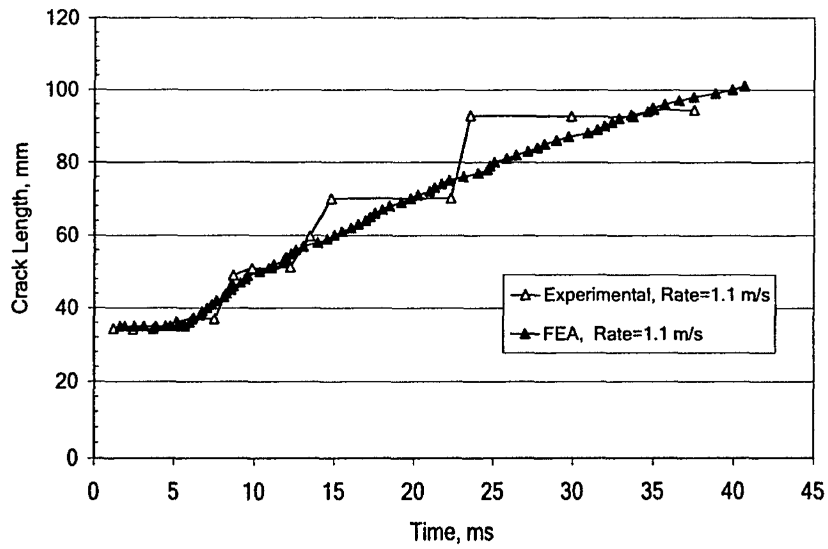

Figure 10. PEEK/carbon-fiber composite FEA and experimental (Blackman et al. 1995; 1996) crack length versus time for a loading rate 1.1 m/s.

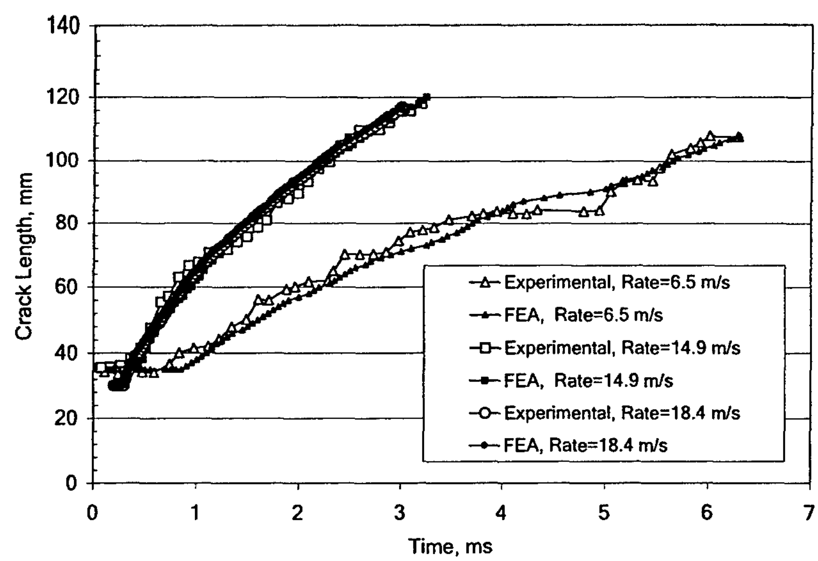

Figure 11. PEEK/carbon-fiber composite FEA and experimental (Blackman et al. 1995; 1996) crack length versus time for loading rates of 6.5, 14.9, and 18.4 m/s.

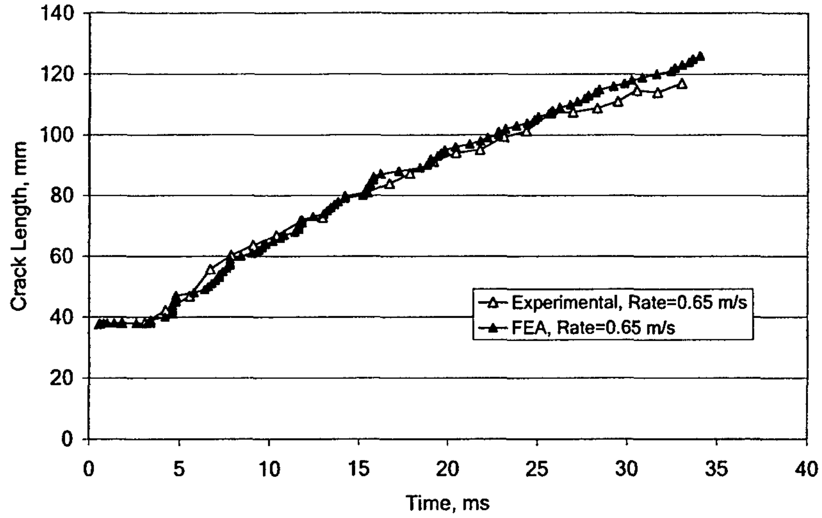

Figure 12. Epoxy/carbon-fiber composite FEA and experimental (Blackman et al. 1995; 1996) crack length versus time for loading rate of 0.65 m/s.

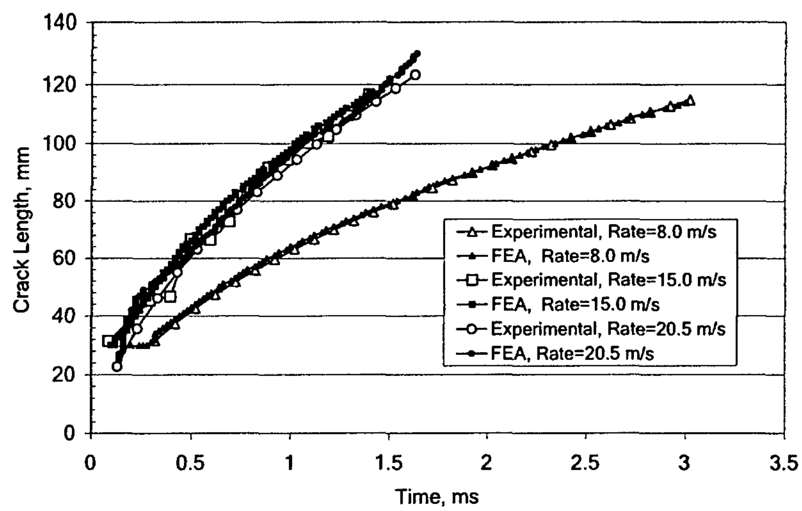

Figure 13. Epoxy/carbon-fiber composite FEA and experimental (Blackman et al. 1995; 1996) crack length versus time for loading rates of 8.0, 15.0, and 20.5 m/s.

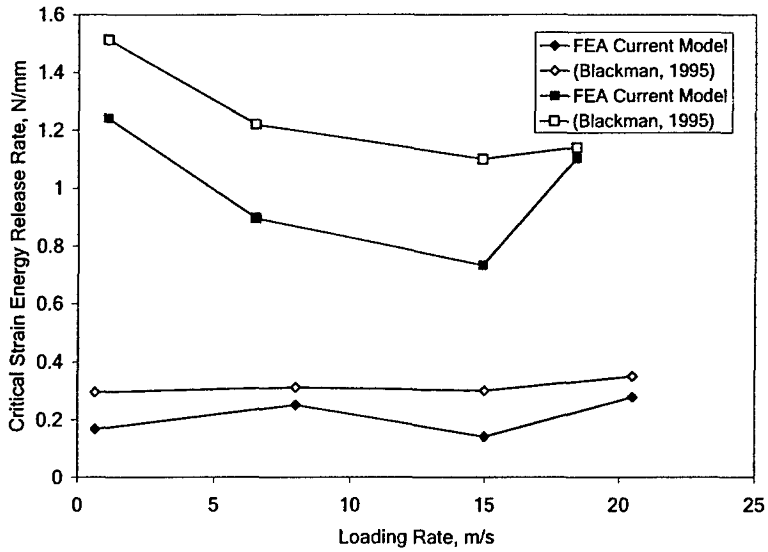

Figure 14. Critical strain energy release rate (Eq. (3)) versus loading rate of rate-independent model ($\nu = \eta = 0$) compared to reported experimental values (Blackman et al. 1995; 1996).

Table 1. Tabulated values of critical strain energy release rate as a function of loading rate for the current rate-independent model ($\nu = \eta = 0$).

Epoxy/Carbon-Fiber		Peek/Carbon-Fiber	
Loading Rate, m/s	Strain Energy Release Rate, N/mm	Loading Rate, m/s	Strain Energy Release Rate, N/mm
0.65	0.168	1.1	1.241
8.0	0.251	6.5	0.897
15.0	0.141	14.9	0.732
20.5	0.278	18.4	1.103

4.1.2 FEA Rate-Dependent Results

An FEA was performed using the rate-dependent cohesive zone model ($\nu \neq 0$ or $\eta \neq 0$). The viscosity terms ν and η and the crack opening parameters u_{cr} and u_{end} were adjusted until agreement between the FEA and experimental crack length versus time curves for the rates analyzed in this study was found. A single set of parameters was desired for all loading rates analyzed. Table 2 presents the rate-dependent cohesive element parameters obtained for the epoxy and PEEK composite materials. As the trend for the PEEK composite material was a decreasing G_c with increasing rate, a negative value of η was required. The viscosity parameter ν was chosen to be zero, as in this particular DCB configuration adjusting its value did not have a significant effect on the overall crack propagation behavior. Figs. 15 and 16 present the crack length versus time curves at each of the loading rates analyzed for the epoxy composite. Good agreement was found between the rate-dependent FEA and the experimental results for loading rates ranging between 0.65and 20.5 m/s. Figures 17 and 18 present the results for the PEEK composite for rates varied from 1.1 to 18.4 m/s. Good agreement between the FEA and experimental results was found. Interestingly, the "stick-slip" crack propagation behavior of the PEEK composite material at a loading rate of 1.1 m/s was captured with this rate-dependent cohesive model. The behavior is also observed at the higher rate of 18.4 m/s as also evidenced in the experimental results. Thus, with the rate-dependent cohesive zone model, a single set of material constants for each material was able to model the rate-dependent behavior of the epoxy and PEEK composites.

Table 2. Rate-dependent model cohesive element parameters.

Parameters	Epoxy/Carbon-Fiber	PEEK/Carbon-Fiber
u_s, µm	0.01	0.01
u_{cr}, µm	0.344	70.0
u_{end}, µm	7.0	100.0
τ_y, GPa	0.0200	0.0200
τ_{max}, GPa	0.0275	0.0275
v, µm/ms	0.0	0.0
η, µm/ms	50.0	-5.30

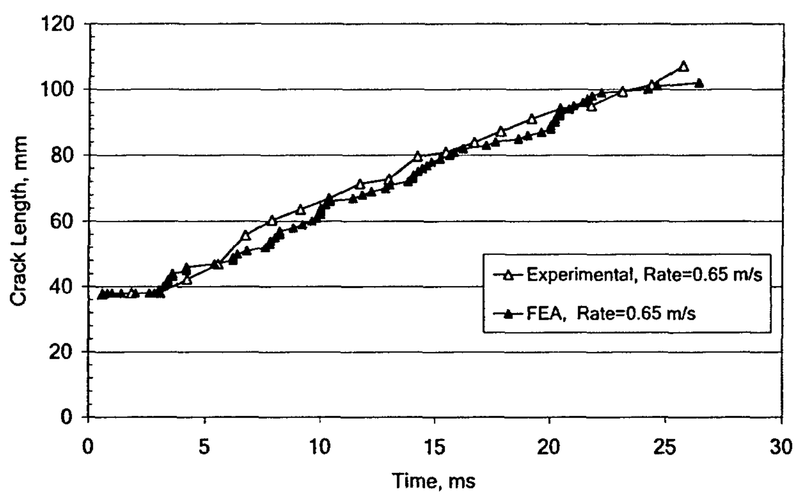

Figure 15. Rate-dependent model results: epoxy/carbon-fiber composite FEA and experimental (Blackman et al. 1995; 1996) crack length versus time for loading rate of 0.65 m/s.

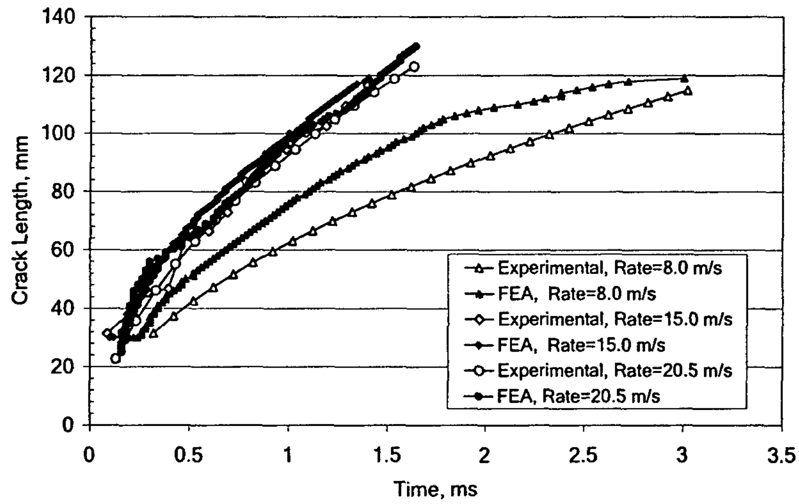

Figure 16. Rate-dependent model results: epoxy/carbon-fiber composite FEA and experimental (Blackman et al. 1995; 1996) crack length versus rime for loading rates of 8.0, 15.0, and 20.5 m/s.

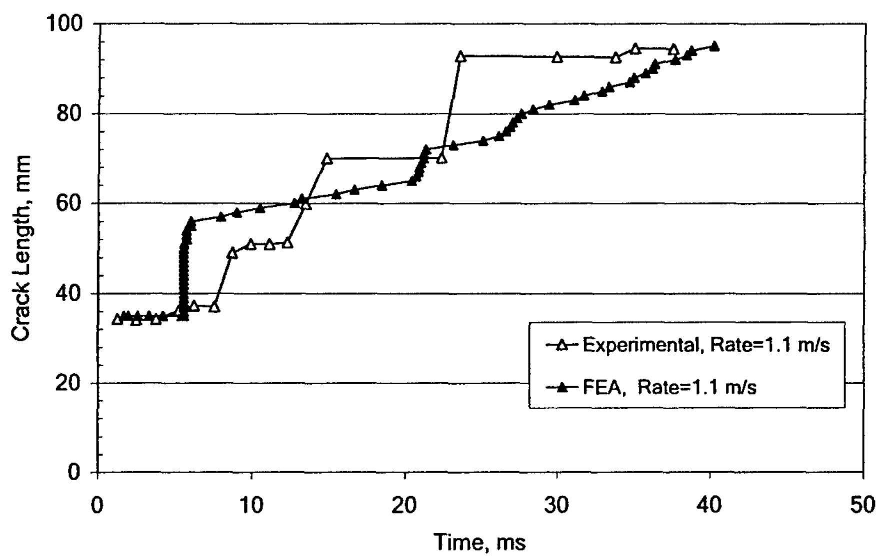

Figure 17. Rate-dependent model results: PEEK/carbon-fiber composite FEA and experimental (Blackman et al. 1995; 1996) crack length versus time for loading rate of 1.1 m/s.

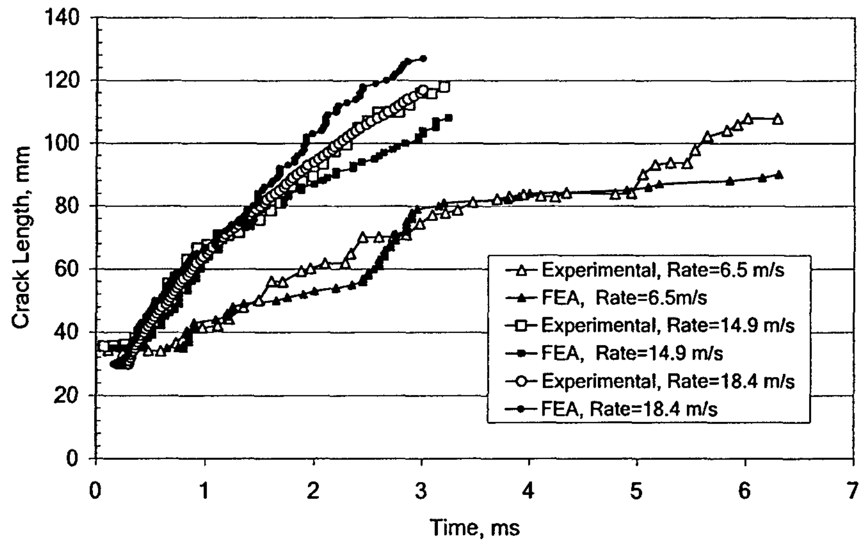

Figure 18. Rate-dependent model results: PEEK/carbon-fiber composite FEA and experimental (Blackman et al. 1995; 1996) crack length versus time for loading rates of 6.5, 14.9, and 18.4 m/s.

4.2 Experimental Results from High Strain Rate Apparatus

The experimental apparatus as described in section 3.1.2 was used to test the DCB experimental specimens described in 3.1.1. The DCB specimens composed of NCT-350-TR-50, obtained from Newport Adhesives & Composites, Inc.

The crack opening displacements along the direction of crack growth and load were collected for 6 specimens. Representative results, crack length, crack velocity, and load time histories, are shown in Figures 19-24. The testing procedure was found to produce loading rates ranging from 0.6 to 14.5 m/s.

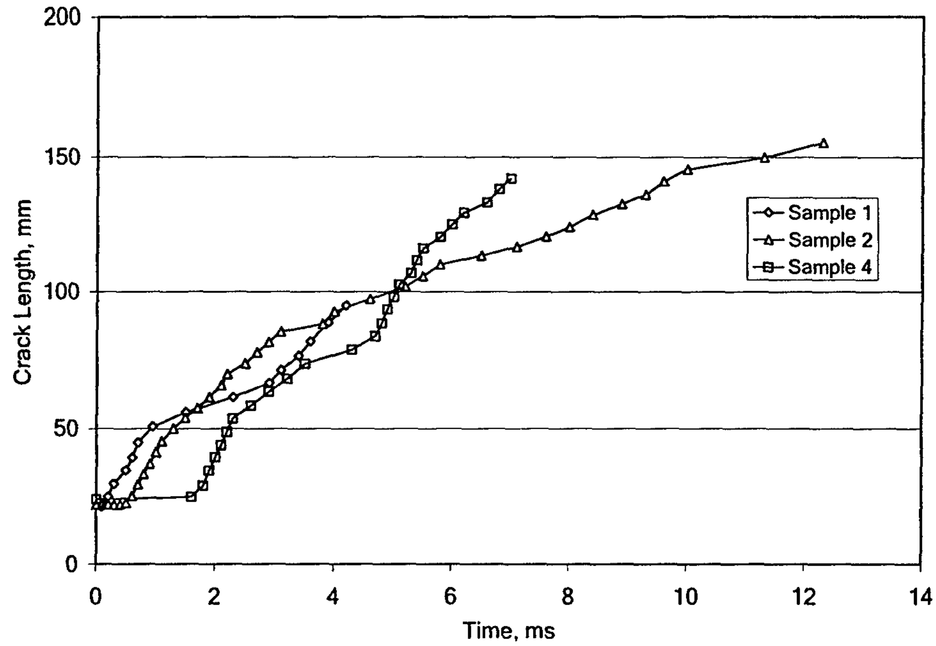

Figure 19. DCB experimental results samples 1, 2, 4: crack length versus time.

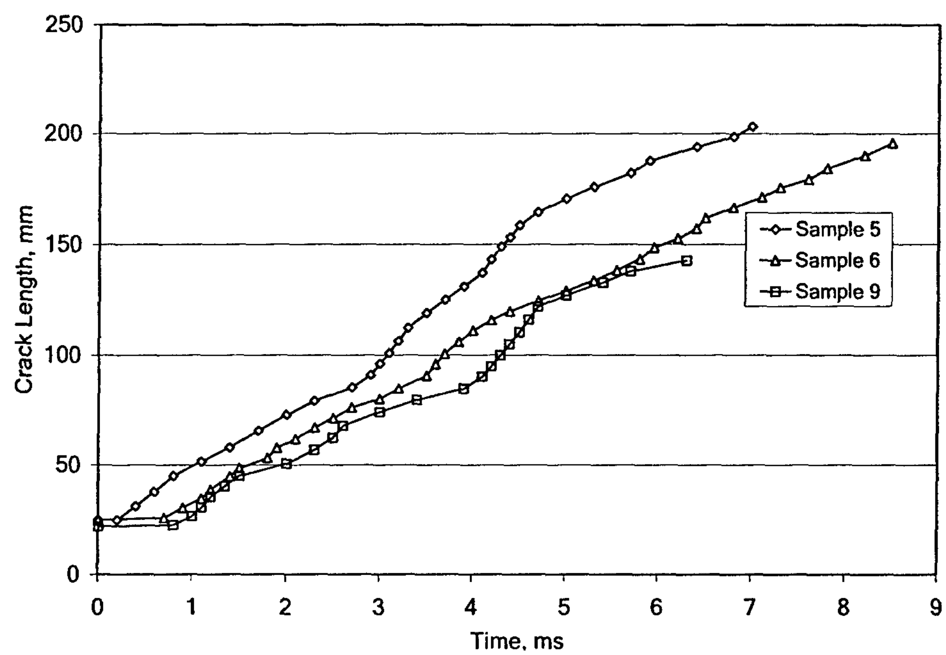

Figure 20. DCB experimental results samples 5, 6, 9: crack length versus time.

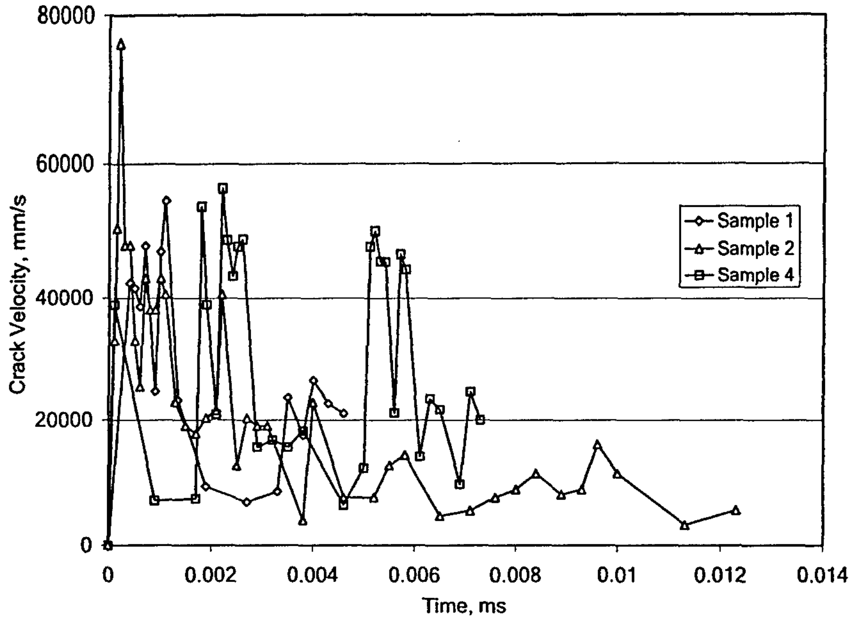

Figure 21. DCB experimental results for samples 1, 2, and 4: crack velocity versus time.

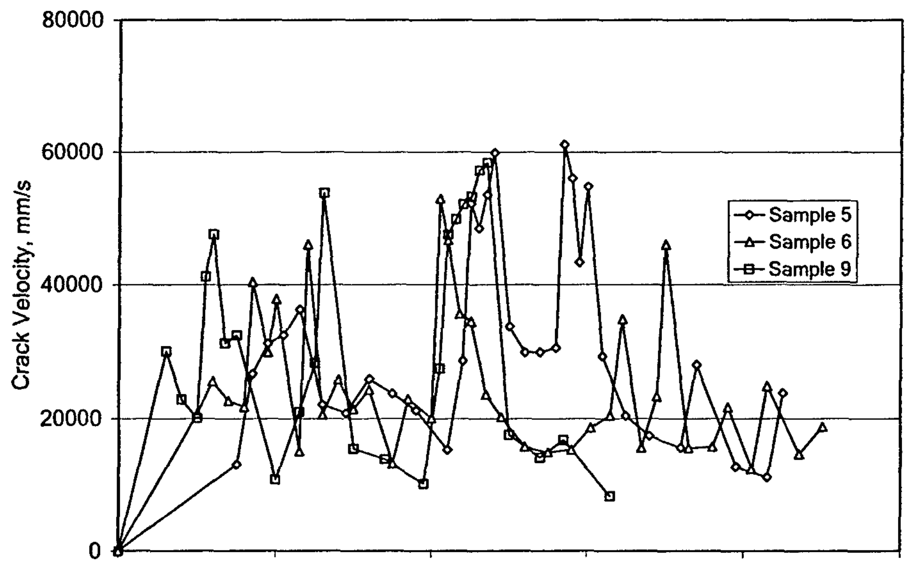

Figure 22. DCB experimental results for samples 5, 6, and 9: crack velocity versus time.

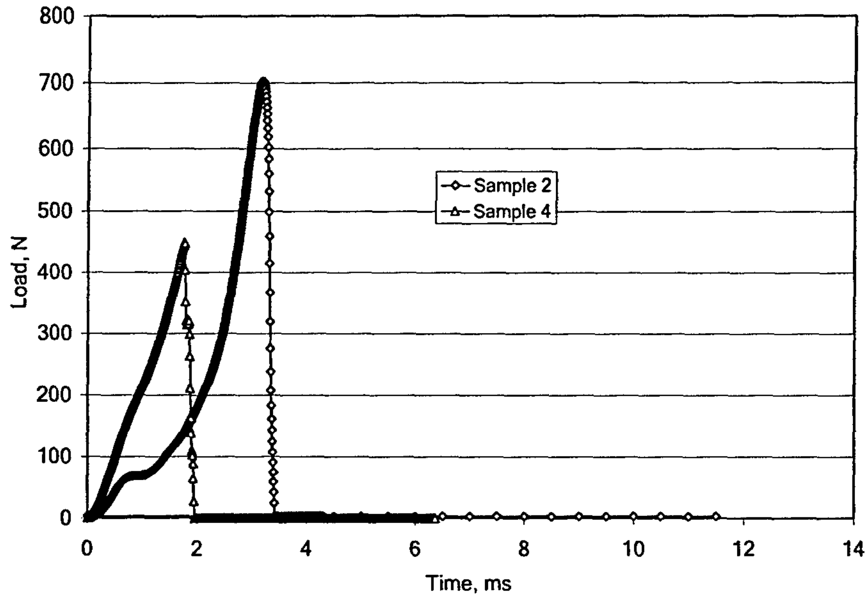

Figure 23. DCB experimental results for samples 2 and 4: measured load versus time.

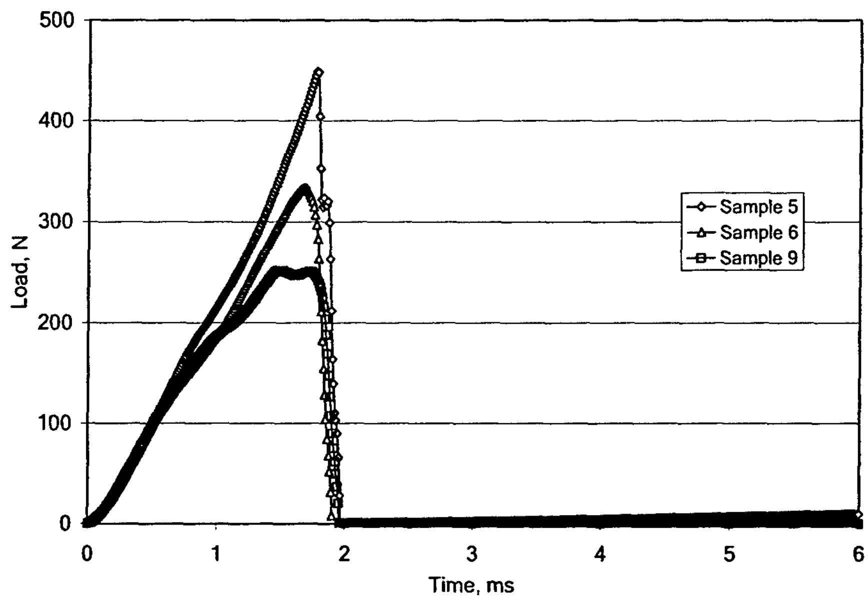

Figure 24. DCB experimental results for samples 5, 6, and 9: measured load versus time.

4.3 Finite Element Analysis of Experimental Results

A finite element analysis simulating testing of the 6 DCB samples (Samples 1, 2, 4, 5, 6, and 9) was performed. The measured crack mouth opening displacements (CMOD) as a function of time are presented in Figures 25-26. Piecewise linear curve fits were performed, in order to obtain the prescribed velocities for the model loading condition. The velocities used are shown in Table 3. The rate-independent cohesive model ($\nu=\eta=0$) was used with a single set of parameters presented in Table 4. These results are presented in Figures 27-28 where comparison of the FEA and experimental results are presented. The cohesive model parameters were chosen so that that good agreement was obtained for Sample 2. Thus, comparing the results of the remaining samples, the rate-independent FEA results don't agree as suspected, indicating a rate-dependent model is required to adequately model this material subjected to high loading rates.

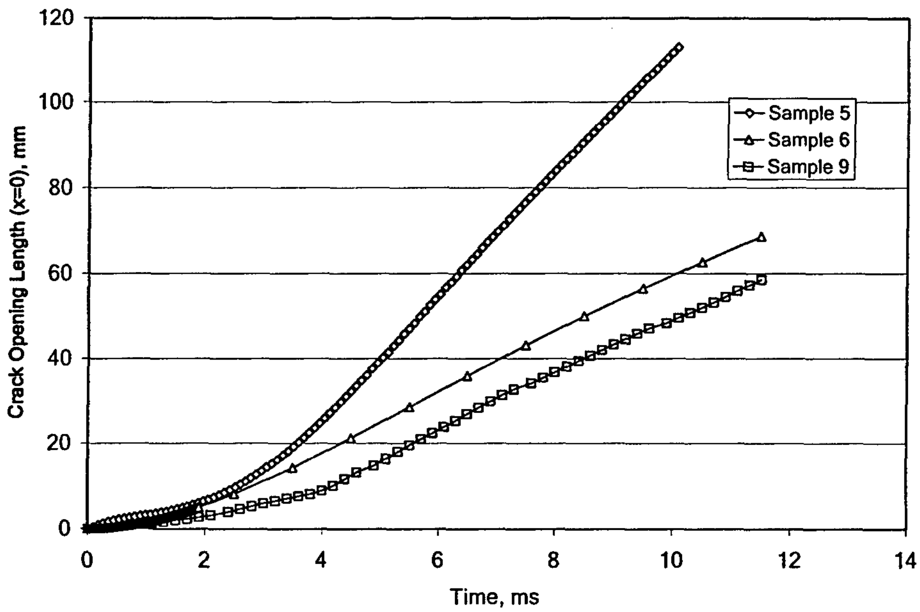

Figure 25. Measured Crack Opening at Specimen End versus time (Samples 1, 2, and 4).

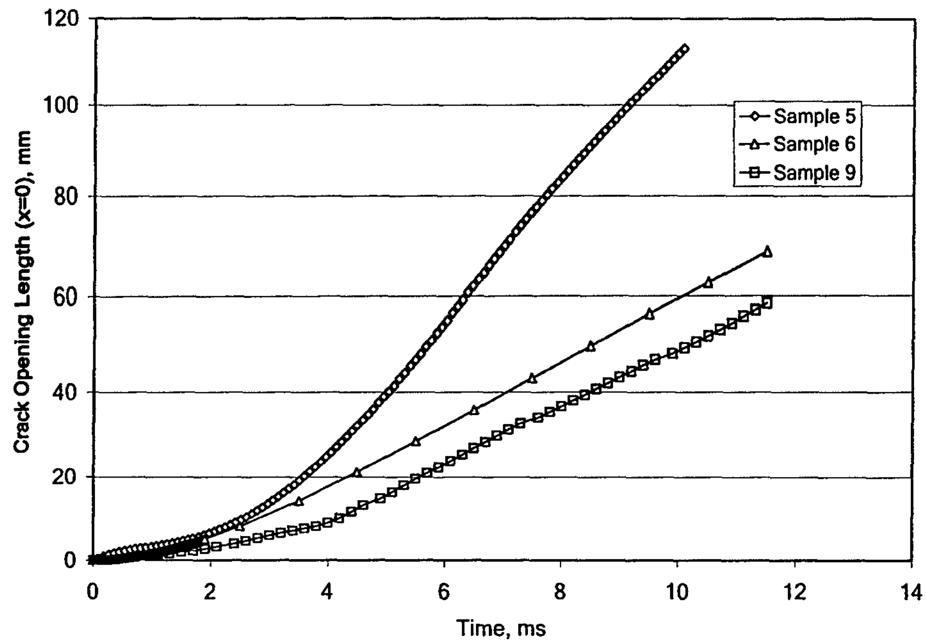

Figure 26. Measured Crack Opening at Specimen End versus time (Samples 5, 6, and 9).

Table 3. Prescribed Velocities Used for FEA of RHAMM DCB Experiments

Sample	Time (ms)	Velocity (mm/ms)
1	0-3.1	3.538
	3.1-7.1	6.968
	7.1-	4.323
2	0-	1.863
4	0-2	0.619
	2-4.5	2.367
	4.5-	4.864
5	0-2	3.941
	2-3.5	8.386
	4.5-	14.484
6	0-2	2.147
	2-	6.813
9	0-4	1.885
	4-	6.590

Table 4. Cohesive element parameters for RHAMM Experiments

	NCT-350-TR-50	
Parameters	Rate-Independent	Rate-Dependent
u_s, µm	0.01	0.01
u_{cr}, µm	0.344	2.0
u_{end}, µm	30	2.5
τ_y, GPa	0.0200	0.0200
τ_{max}, GPa	0.0275	0.0275
ν, µm/ms	0.0	0.0
η, µm/ms	0.0	220

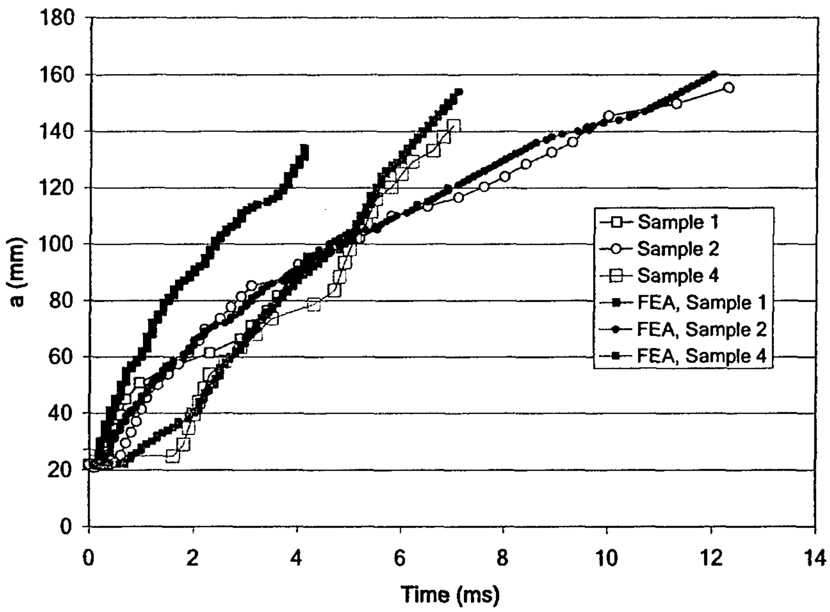

Figure 27. Comparison of DCB Rate-Independent FEA to experimental (samples 1, 2, and 4): crack length versus time.

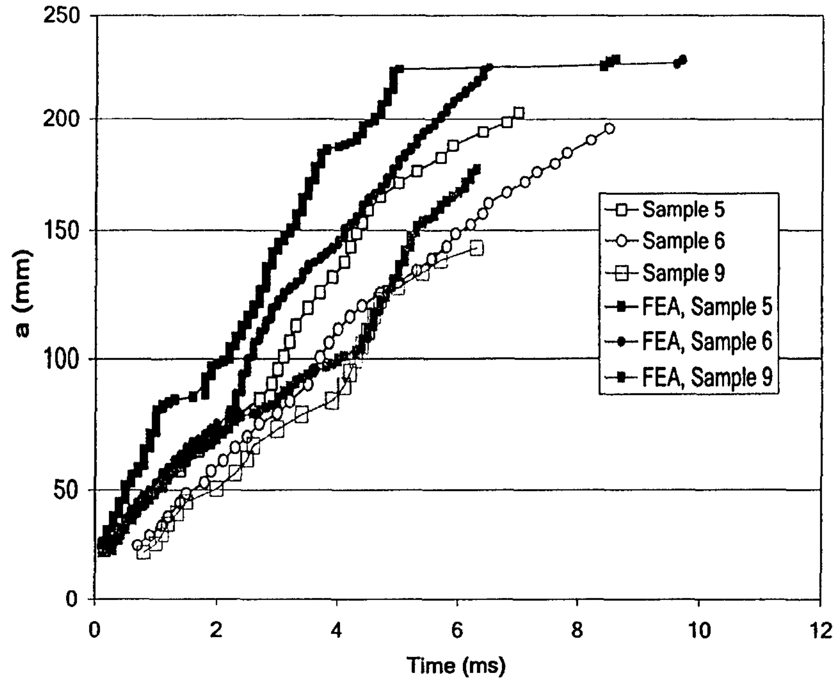

Figure 28. Comparison of DCB Rate-Independent FEA (samples 5, 6, and 9) to experimental: crack length versus time.

The rate-dependent cohesive model ($\eta \neq 0$) was then used with a single set of parameters presented in Table 3. A comparison of the rate-dependent FEA results to the experimental results are presented in Figures 29-30. Although the agreement was not perfect, much better agreement was found with the rate-dependent model compared to the rate-independent model.

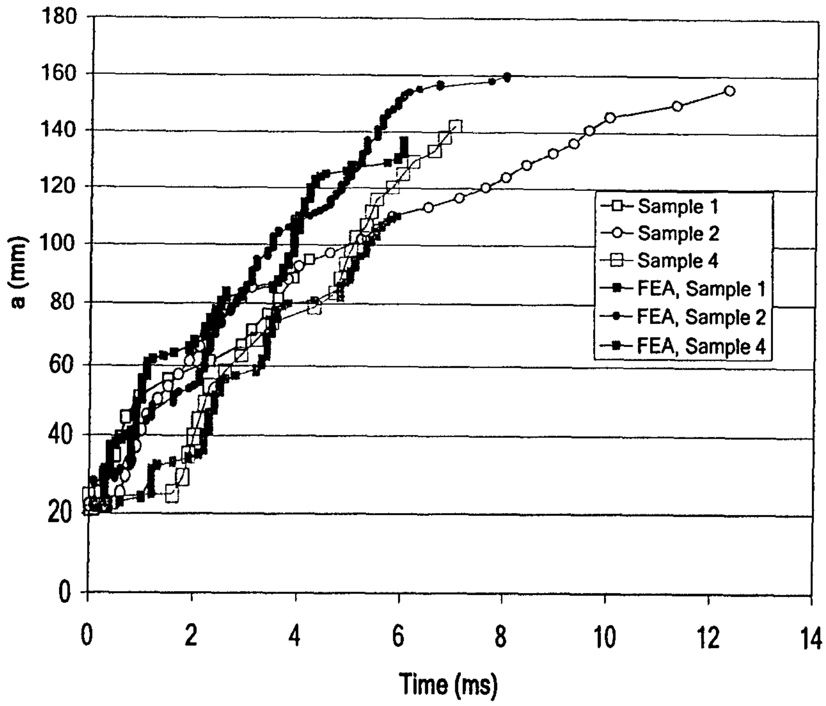

Figure 29. Comparison of DCB Rate-Dependent FEA to experimental (samples 1, 2, and 4): crack length versus time.

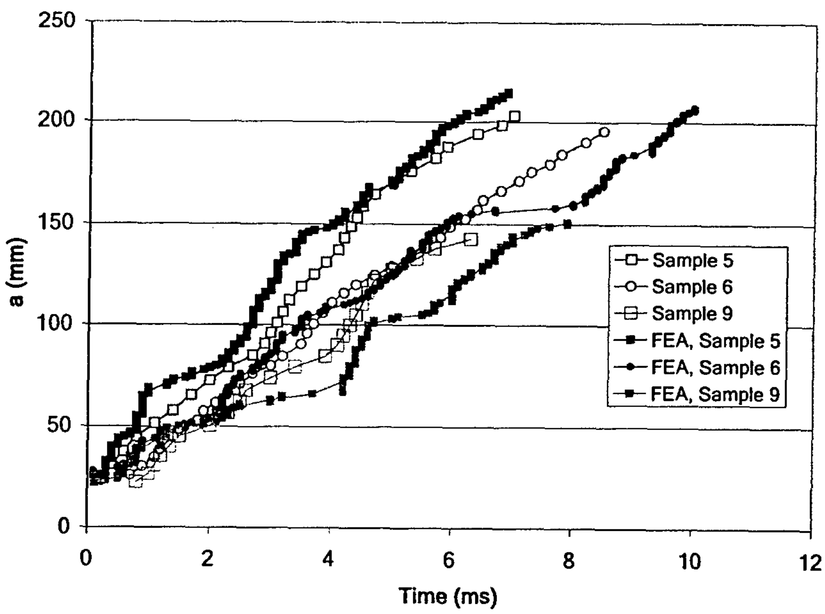

Figure 30. Comparison of DCB Rate-Dependent FEA (samples 5, 6, and 9) to experimental: crack length versus time.

5 Conclusions

The unique rate-dependent cohesive zone model presented in this paper was implemented using the user defined cohesive material model of LS-DYNA and was used to model published experimental mode I testing of epoxy and PEEK / carbon-fiber composites at varied loading rates. With a rate-independent model, agreement of the published experimental data and the FEA at varied loading rates was obtained only by increasing the critical strain energy release rate. The rate-dependent model, with a single set of constants for each composite material, good agreement between the FEA and previously published experimental results was found over the loading rates considered. "Stick-slip" crack growth behavior observed experimentally at specific rates was also captured.

The rate-dependent model developed during this research is unique as it contains a rate-dependent term for the onset of the opening ($\nu\dot{u}$) of the cohesive zone combined with a maximum traction rate-dependent term ($\dot{u}\eta$). The model is also unique in that a cohesive zone starting or yielding displacement (u_s) may be defined to greatly increase numerical stability.

To the author's knowledge this is the first time a rate-dependent cohesive model has been implemented into a commercial code for both shells and bricks and has been validated with experimental data at varied loading rates. Additionally with the addition of the yield displacement (u_s), this method was found to be computationally robust.

A simple inexpensive testing apparatus was developed for high rate DCB testing. With this apparatus, samples may be subjected to varied 0.6 to 14.5 mm/s. FEA of experiments performed using this apparatus showed that the rate-dependent cohesive model is necessary to adequately model the composite material tested (NCT-350-TR-5). Thus, using this apparatus the material parameters needed for the rate-dependent cohesive zone model may be determined with a small number of experiments (<10).

The rate-dependent cohesive zone model and experimental apparatus developed in this project have been shown to be viable for use of accurately predicting the survivability of multi-sparred, fuel-filled composite wing structures.

6 Recommendations

For extension of this work, it is recommended to expand the mode I rate-dependent cohesive element validated in this work to include mode II and mixed mode rate-dependent behavior. This model would be validated for pure mode II using simple double cantilever beam specimens and for mixed mode (mode I and II) using real composite wing joints. Numerical results should be matched with experimental results with varied rates consistent with hydrodynamic ram. Multiple joint geometries and materials should be considered for this validation.

References

Blackman, B. R. K., Dear, J. P., Kinloch, A. J., MacGillivray, H., Wang, Y., Williams J. G., and Yayla, P. (1995). "The failure of fibre composites and adhesively bonded fibre composites under high rates of test: part I mode I loading-experimental studies." *Journal of Materials Science,* 30, 5885-5900.

Blackman, B. R. K., Kinloch, A. J., Wang, Y., and Williams J.G. (1996). "The failure of fibre composites and adhesively bonded fibre composites under high rates of test: part II mode I loading-dynamic effects." *Journal of Materials Science*, 31, 4451-4466.

Camanho, P. P., Dávila, C. G. (2004). "Fracture analysis of composite co-cured structural joints using decohesion elements." *Fatigue Fract. Engng. Mater. Struct.,* 27, 745-757.

Chowdhury, S. R., and Narasimhan, R. (2000). "A cohesive finite element formulation for modeling fracture and delamination in solids." *Sādhanā,* 25(6), 561-587.

Costanzo, F., and Walton, J. R. (1997). "A study of dynamic crack growth in elastic materials using a cohesive zone model." *Int. J. Engng. Sci.,* 35(12/13), 1085-1114.

Fager, L.-O., Bassani, J. L., Hui, C.-Y., and Xu, D.-B. (1991). "Aspects of cohesive zone models and crack growth in rate-dependent materials." *Int. J. of Fracture,* 52, 119-144.

Glennie, E. B. (1971). "A strain-rate dependent crack model." *J. Mech. Phys. Solids,* 19, 255-272.

Kubair, D. V., Geubelle, P. H., and Huang, Y. Y. (2003). "Analysis of a rate-dependent cohesive model for dynamic crack propagation." *Eng. Fracture Mechanics,* 70, 685-704.

La Saponara, V., Muliana, H., Haj-Ali, R., and Kardomateas, G. A. (2002). "Experimental and numerical analysis of delamination growth in double cantilever laminated beams." *Eng. Fracture Mechanics,* 69, 687-699.

Rahul-Kumar, P., Jagota, A., Bennison, S. J., and Saigal, S. (2000). "Cohesive element modeling of viscoelastic fracture: application to peel testing of polymers." *Int. J. of Solids and Structures,* 37, 1873-1897.

Ruiz, G., Pandolfi, A., and Ortiz, M. (2001). "Three-dimensional cohesive modeling of dynamic mixed-mode fracture." *Int. J. Numer. Meth. Engng.,* 52, 97-120.

Tvergaard, V., and Hutchinson, J. W. (1996). "Effect of strain-dependent cohesive zone model on predictions of crack growth resistance." *Int. J. Solids Structures,* 33(20-22), 3297-3308.

Xu, D.-B., Hui, E. J., Kramer, E. J., and Creton, C. (1991). "A micromechanical model of crack growth along polymer interfaces." *Mechanics of Materials* 11, 257-268.

Appendixes

A1. List of Personnel Involved in Work

The following researchers at RHAMM Technologies, LLC were involved in this work:

Dr. Monty A. Moshier, Principle Investigator
Dr. Ronald L. Hinrichsen, Chief Engineer
Dr. Brian D. Choules, Senior Engineer
Mr. Steve Stratton, Engineering Analyst
Brian J. Barlow, Engineering Analyst

A2. Publications

M. A. Moshier, R. L. Hinrichsen, G. Czarnecki, D. Barrett, M. Weisenbach, "Dynamic Loading Methodologies," 43rd AIAA/ASME/ASCE/AHS SDM Conference, 22 - 25 Apr 2002, Denver, Colorado.

M. A. Moshier, R. L. Hinrichsen, G.J. Czarnecki, "Dynamic Loading Methodologies," AIAA Journal, Vol. 41, Number 11, PP 2291-2294, Nov. 2003.

M. A. Moshier, R. L. Hinrichsen, G. Czarnecki, N.L. Cook, "Testing Composite Joints Under High Energy Hydrodynamic Ram Conditions," 45th AIAA/ASME/ASCE/AHS SDM Conference,19-23 Apr 2004, Palm Springs, CA.

B.D. Choules, M.A. Moshier, and R.L. Hinrichsen, "High Strain Rate Failure of Composite Interfaces," 46th AIAA/ASME/ASCE/AHS/ASC Structures, Structural Dynamics & Materials Conference, 18 - 21 Apr 2005, Austin, TX.

B. D. Choules, M. A. Moshier, and R. L. Hinrichsen, "Rate-dependent Cohesive Zone Model for Composite Interfaces," submitted to ASCE Journal of Aerospace Engineering November 2005.

A3. DCB High Rate Experimental Apparatus Drawings

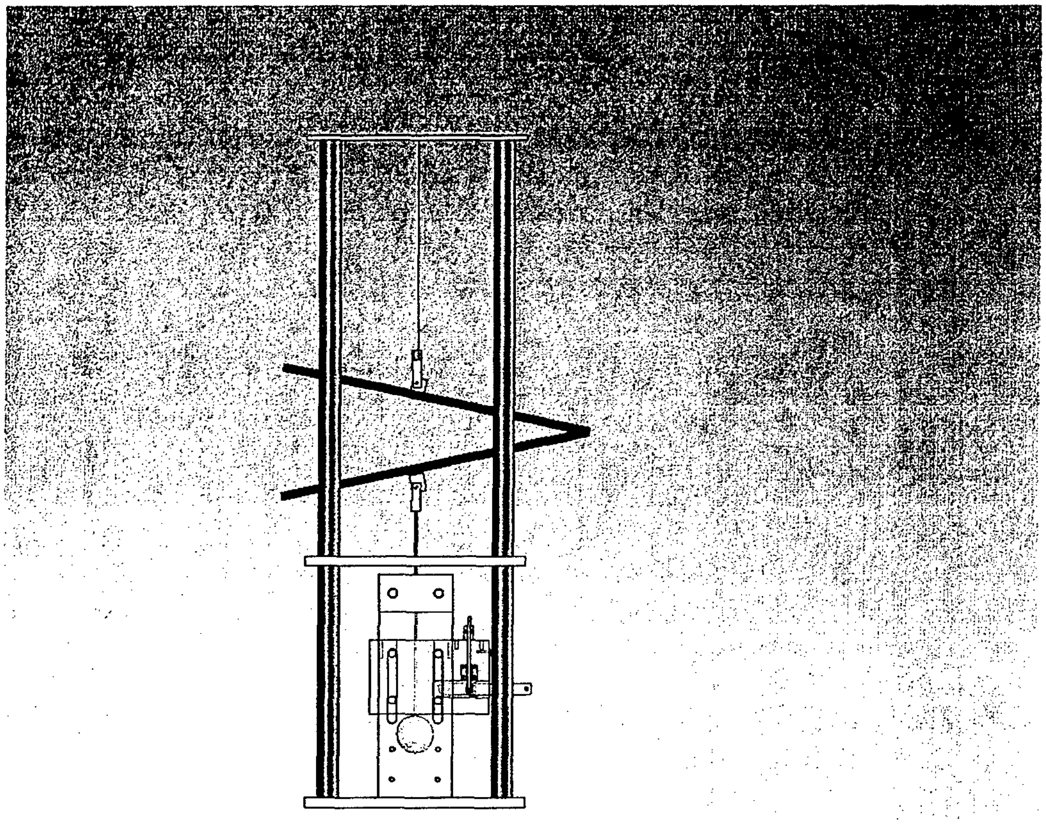

Figure A3-1. Assembly Drawing of DCB High Rate Experimental Apparatus: Side View

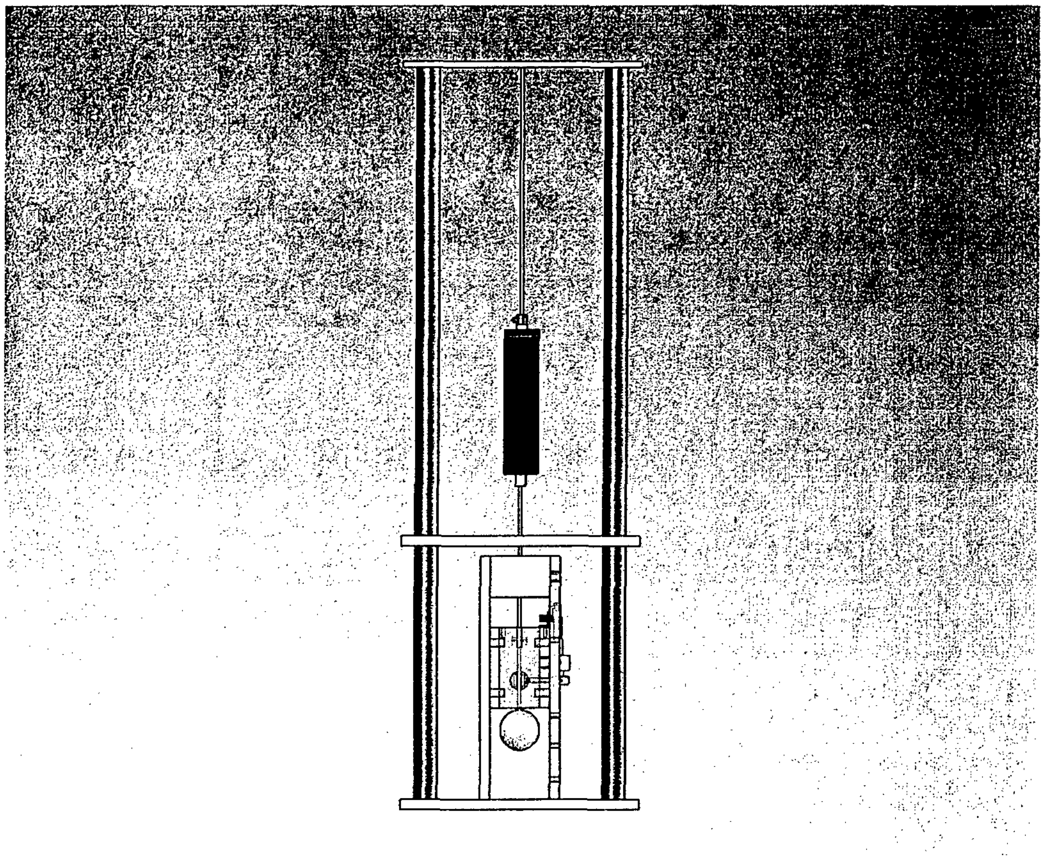

Figure A3-2. Assembly Drawing of DCB High Rate Experimental Apparatus: Front View.

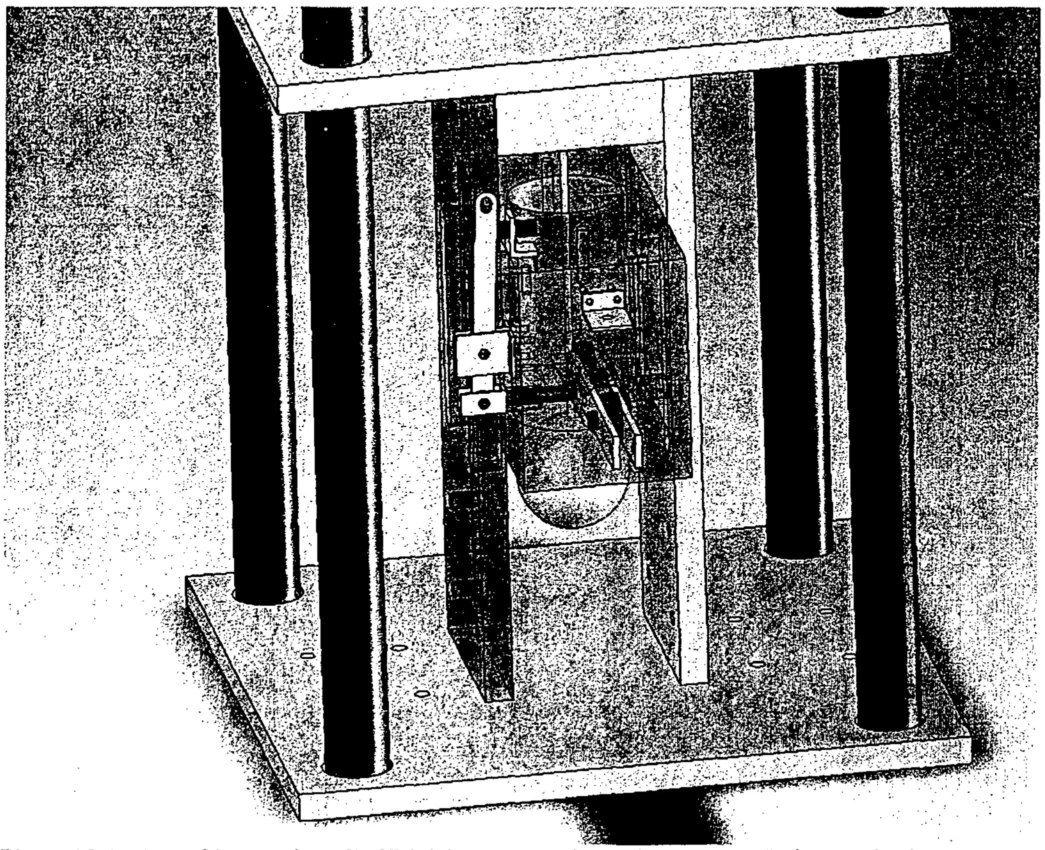

Figure A3-3. Assembly Drawing of DCB High Rate Experimental Apparatus: Spring Mechanism.

Table A3-1: List of Parts

part	material	min dimension	qty
bearings			3
plates	AL	.25x12x12	3
subframe	al	12x3x4	2
framepost	al	13xd.75	8
bolts		1/4-28 x1in	18
bolts		1/2-20 x1	20
springhousing		flange / pipe	1
springblock	al	2x3x4	1
pinblock	al	3x4x6	1
arms	steel	5.5x5x.0625	1
slider	al	hollow ball	1
bolts		12-28 x.5in	10
bolts		12-28 x1in	3
pullpin	al	d.25x1.75	1
nuts		size 1-12	20

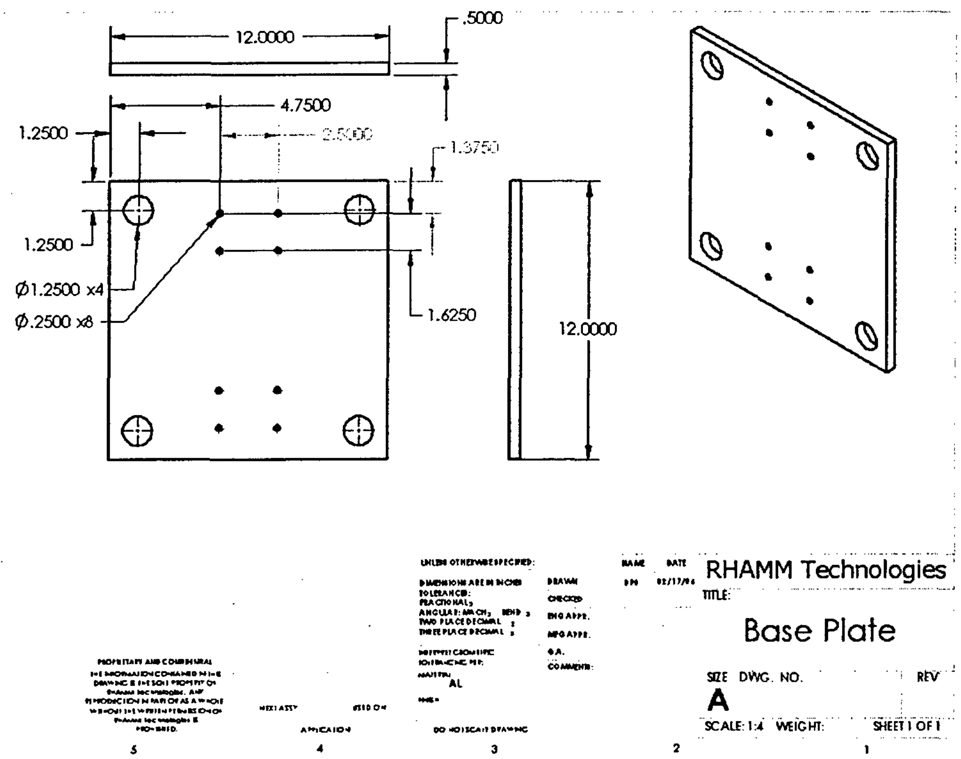

Figure A3-4. Drawing for DCB High Rate Experimental Apparatus: Base Plate.

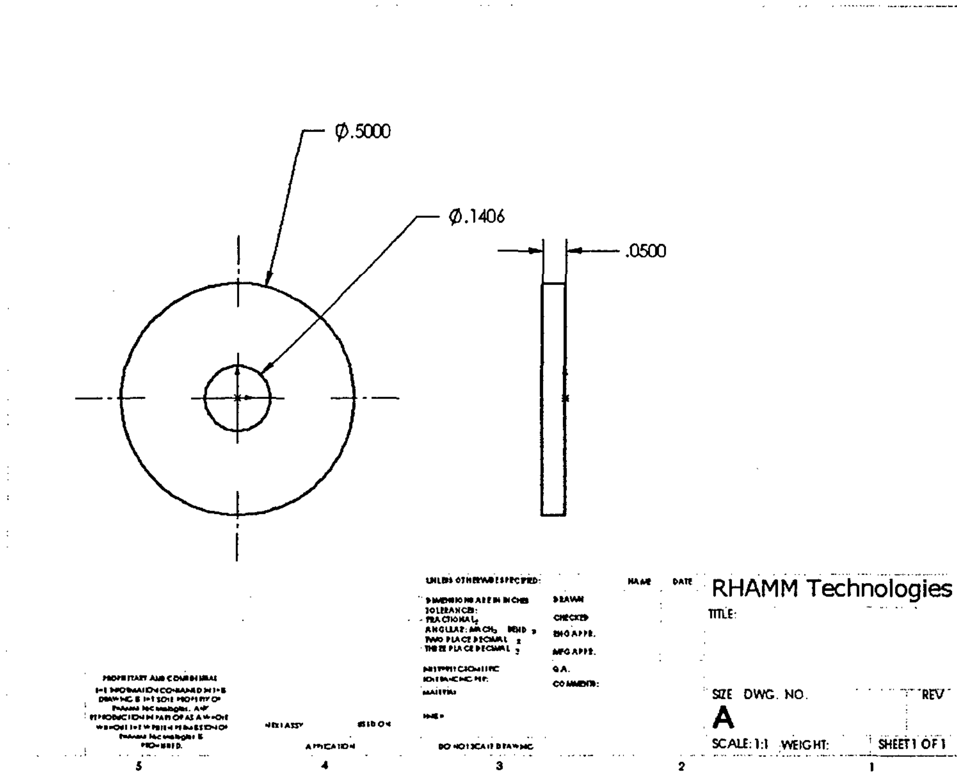

Figure A3-5. Drawing for DCB High Rate Experimental Apparatus: Large Washer.

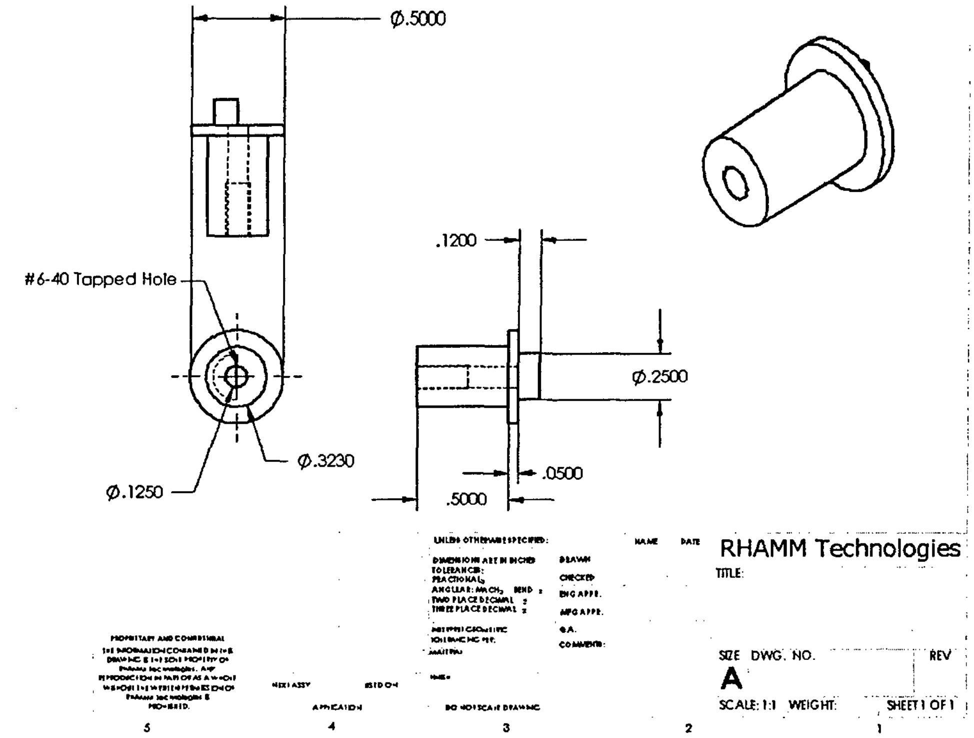

Figure A3-6. Drawing for DCB High Rate Experimental Apparatus: Plug.

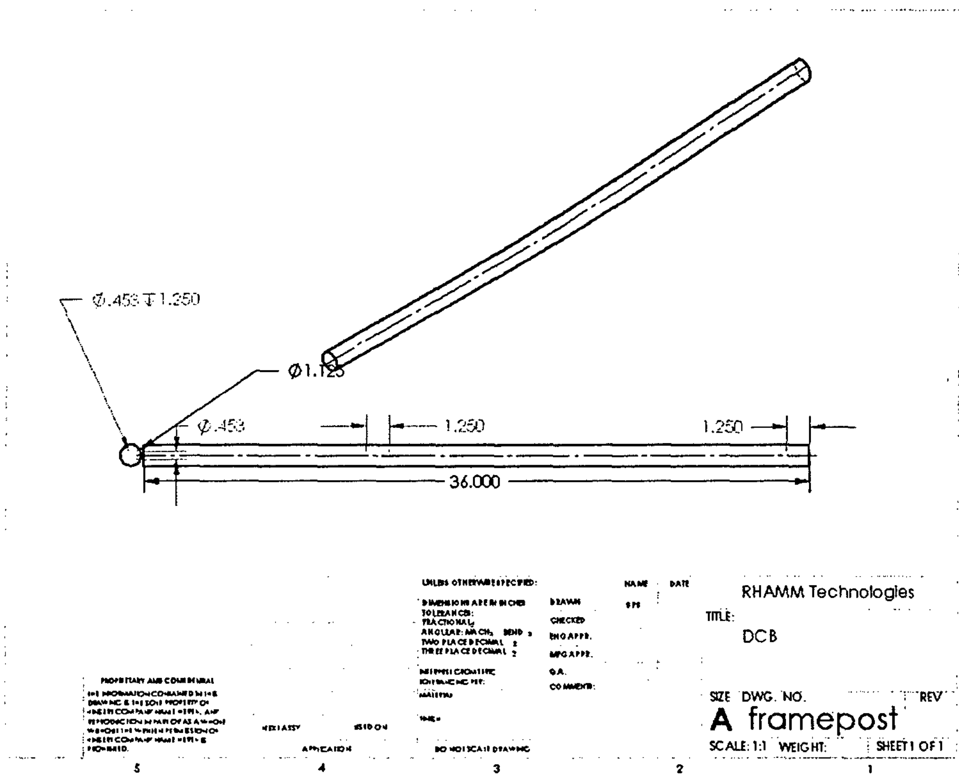

Figure A3-7. Drawing for DCB High Rate Experimental Apparatus: Framepost.

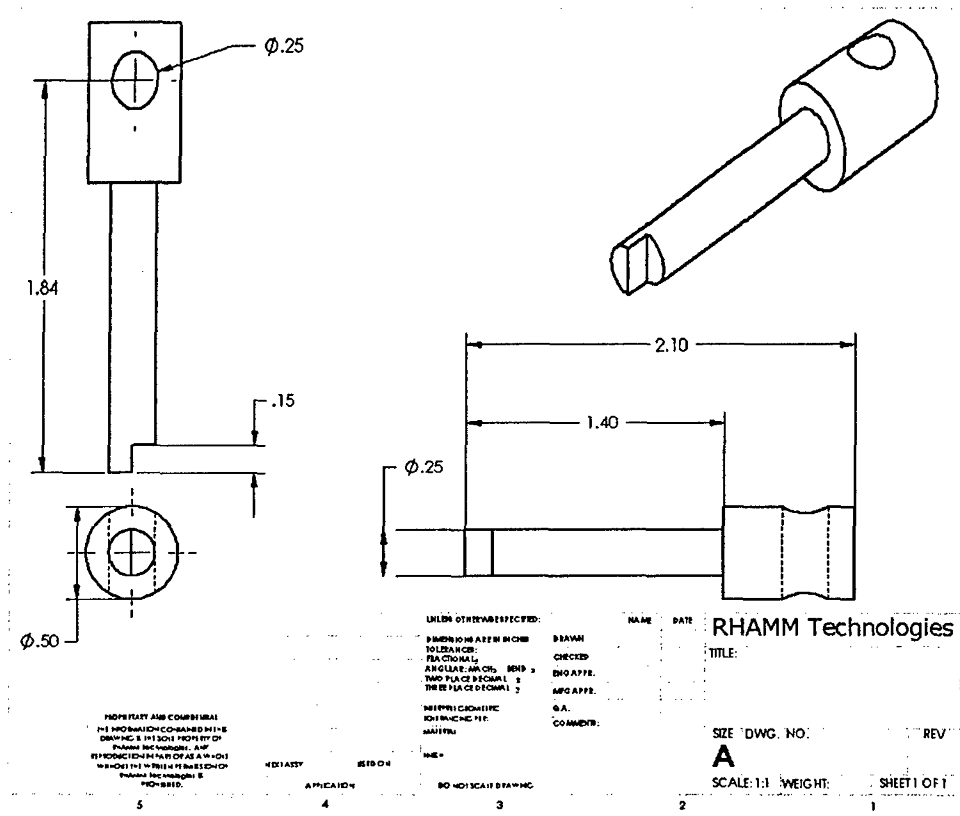

Figure A3-8. Drawing for DCB High Rate Experimental Apparatus: Turnkey.

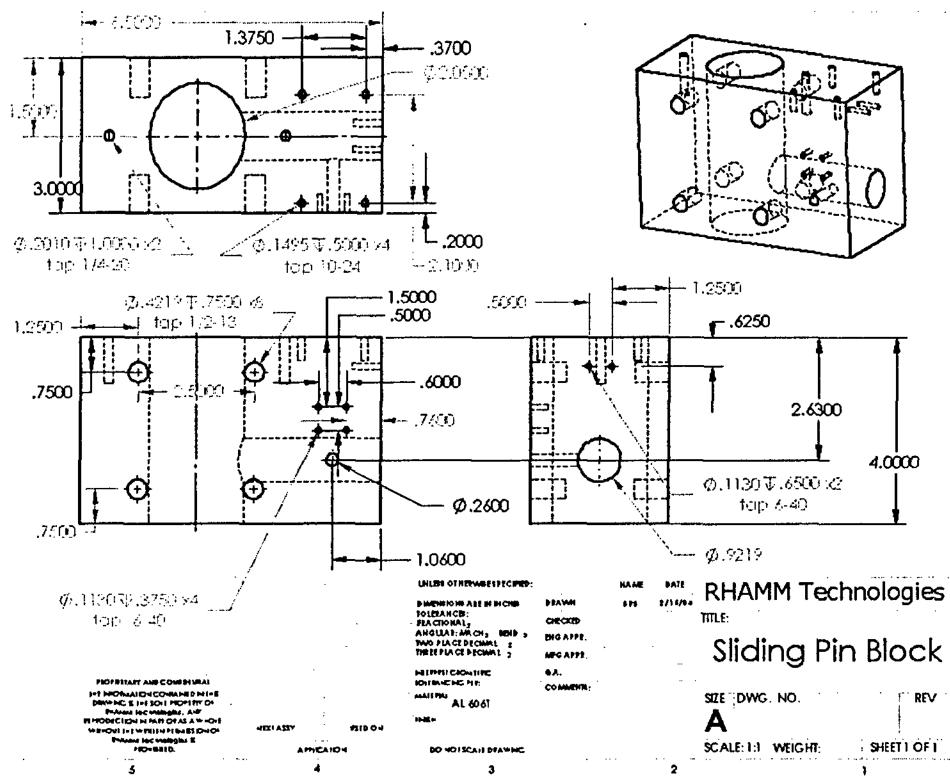

Figure A3-9. Drawing for DCB High Rate Experimental Apparatus: Sliding Pin Block.

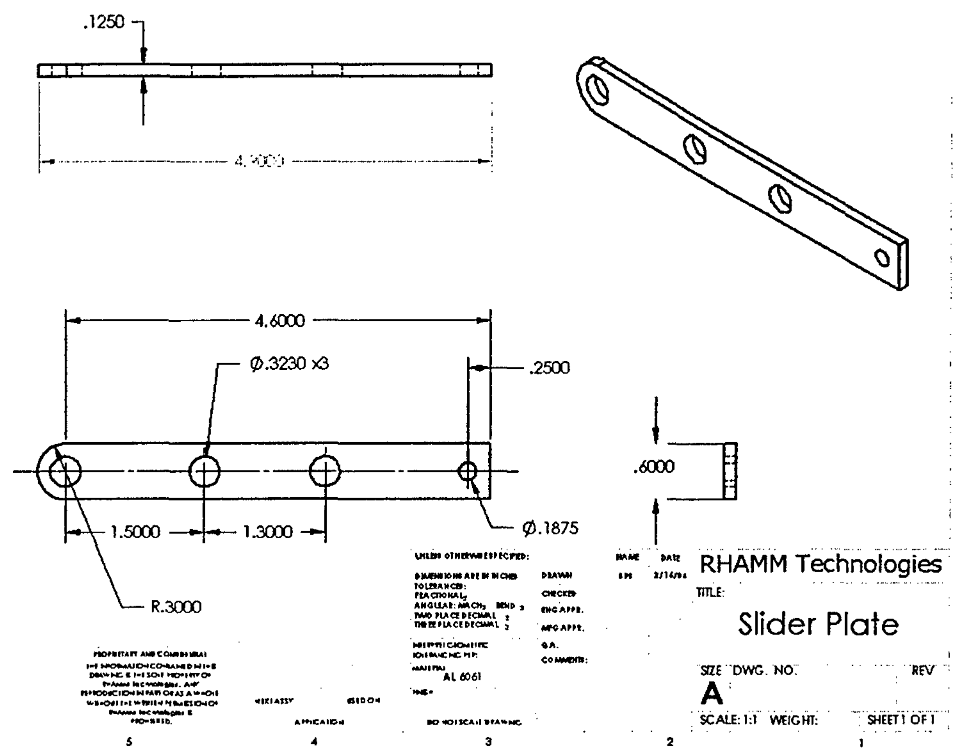

Figure A3-10. Drawing for DCB High Rate Experimental Apparatus: Slider Plate.

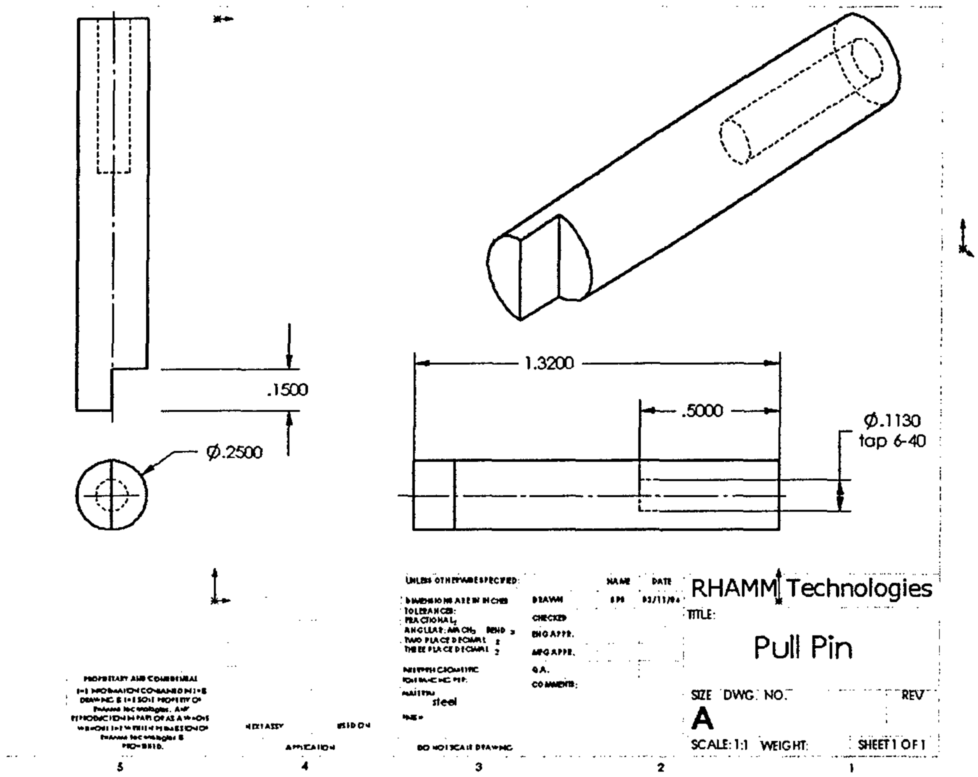

Figure A3-11. Drawing for DCB High Rate Experimental Apparatus: Pull Pin.

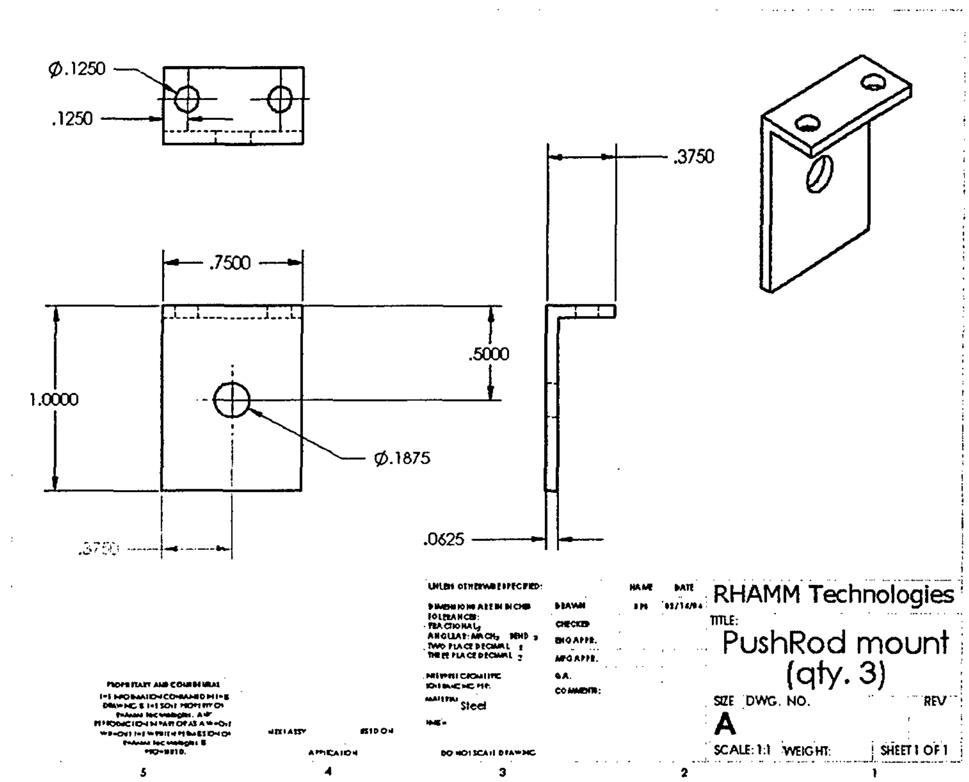

Figure A3-12. Drawing for DCB High Rate Experimental Apparatus: PushRod Mount.

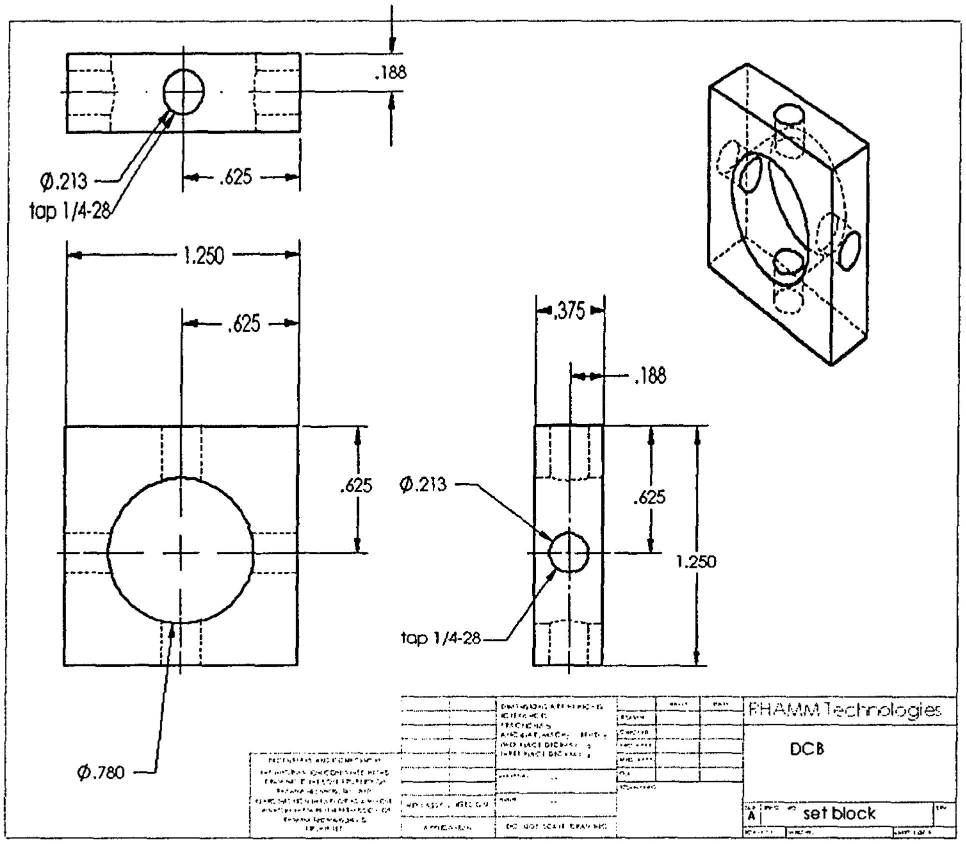

Figure A3-13. Drawing for DCB High Rate Experimental Apparatus: Set Block.

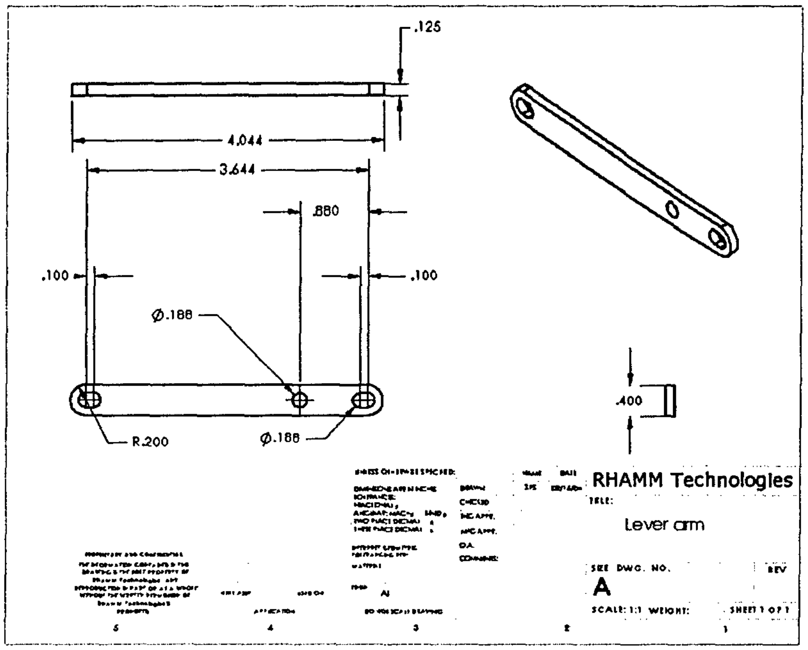

Figure A3-14. Drawing for DCB High Rate Experimental Apparatus: Lever Arm.

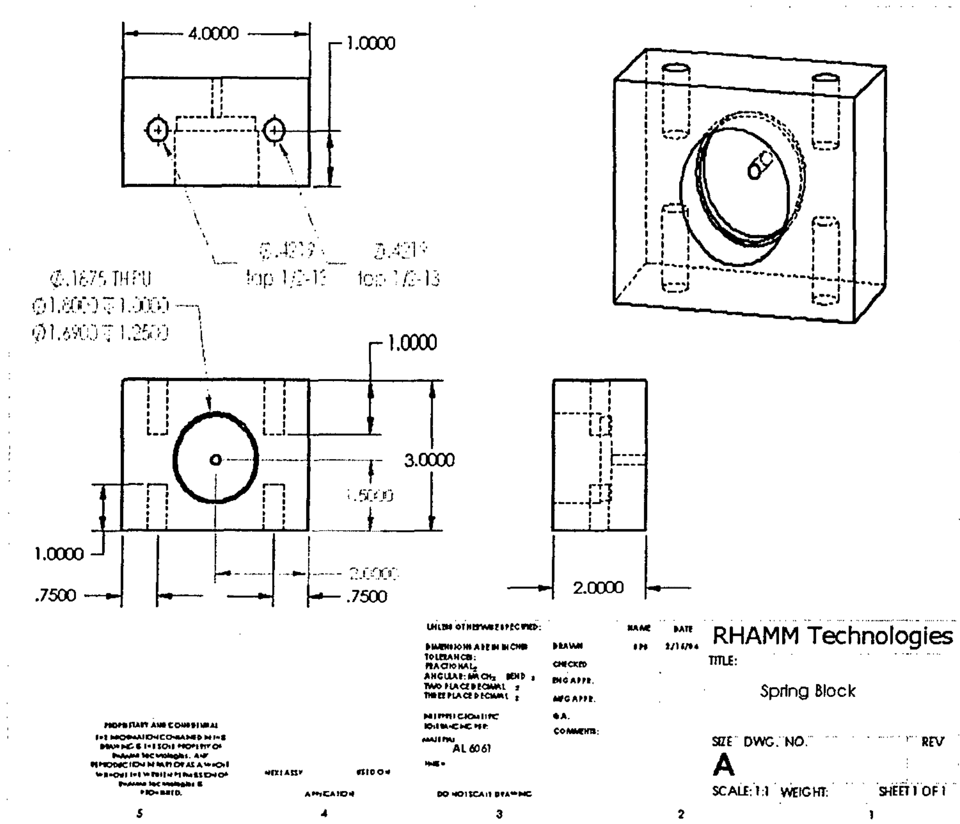

Figure A3-15. Drawing for DCB High Rate Experimental Apparatus: Spring Block.

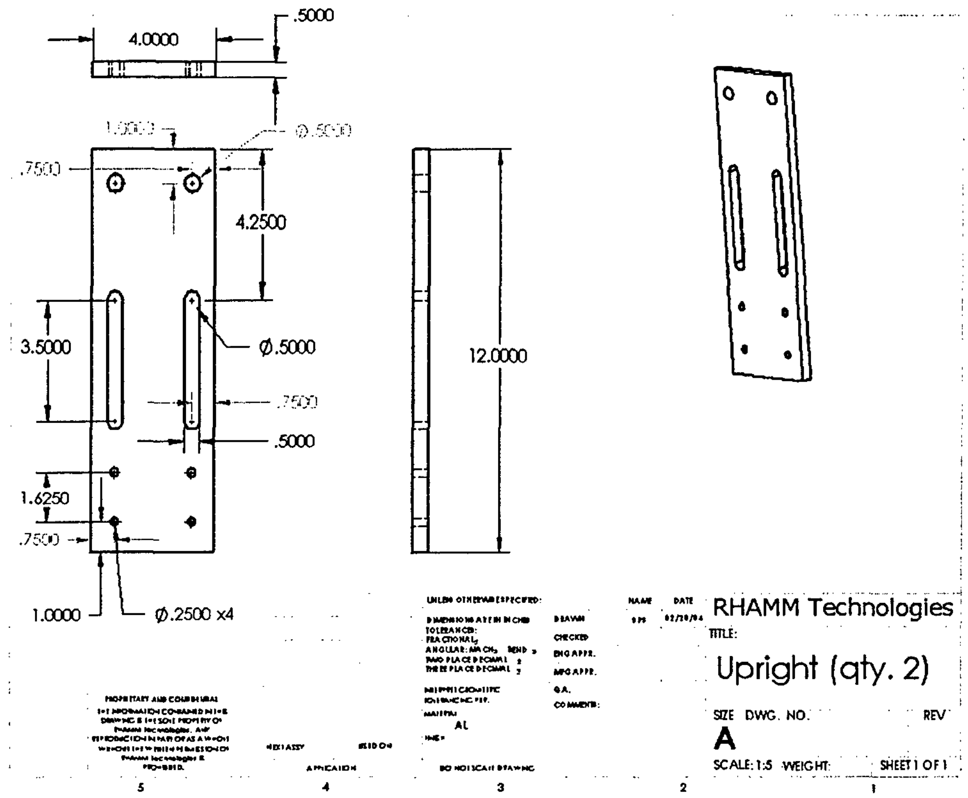

Figure A3-16. Drawing for DCB High Rate Experimental Apparatus: Upright.

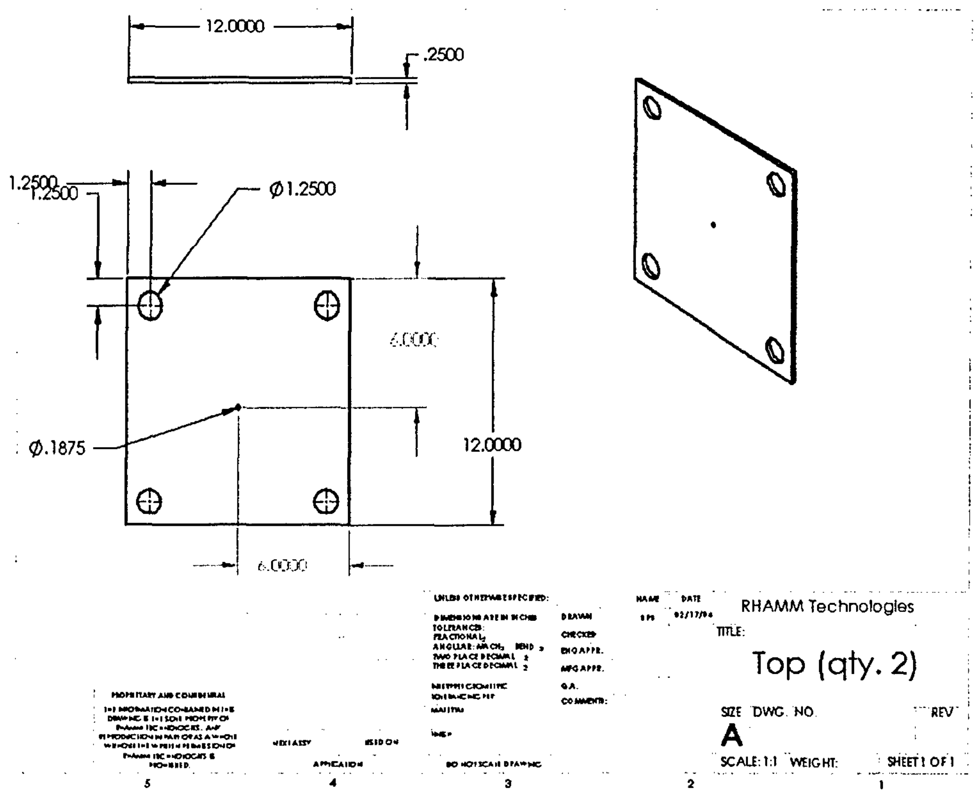

Figure A3-17. Drawing for DCB High Rate Experimental Apparatus: Top.

A4. LS-DYNA User Cohesive Model Code

```
*MAT_USER_DEFINED_MATERIAL_MODELS
$$
$#     mid        ro        mt       lmc       nhv    iortho     ibulk
         1 1.5400E-6        42        15         6
$#   ivect     ifail    itherm    ihyper      ieos
         1         1         0        -1
$#   ROFLG   INTFAIL       u1s     u1int     u1end    syield      smax
sfrac
     0.000  1.000000   1.00E-5 3.4400E-4   0.03000     0.025    0.0275
10.0
$#   etacs     nubdc        kp      ckm2     u2int     u2end      fpen
     0.000       0.0       1.0      80.0 3.4400E-4     0.020      0.01
```

```
      subroutine umat42c(idpart,params,lft,llt,fTraction,jump_u,dxdt,
     &                   aux,ek,ifail,dt1siz,crv)
      include 'nlqparm'
c
c     Rate-Dependent Vectorized Cohesive Material Uer Model
c     Novemeber 15, 2005
c
c     Brian D. Choules, Ph.D
c     RHAMM Technologies
c     332 Skyland Drive
c     Bellbrook OH 45305-8717
c
c Inputs
c    Mode I parameters
c      u1s    = displacement for syield
c      u1int  = displacement at start of damage, ucr
c      u1end  = displacement at end of damage, uend
c      syield = yield stress at u=u1s
c      smax   = maximum stress at ucr and dudt=0
c      sfrac  = fracture Stress
c      etacs  = viscosity parameter for smax
c      nubdc  = viscosity parameter for syield
c      Kp     = gain parameter for keeping nodes together when not
yielded
c    Mode II and III parameters
c      ckm2   = stiffness mode II and III
c      u2int  = mode II and  III critical displacment
c      u2end  = mode II and  III end displacement
c    Other Input
c      fpenalty = constant for resisting penetration
c
c***  variables
c          idpart    =  part ID
c          params    = material constants
c          lft,llt   = start and end of block
c          fTraction = components of the cohesive force
c          jump_u    = components of the displacement
```

```
c          dxdt      = components of the velocity
c          aux       = history storage
c              aux(i,1) =storage for yielding condition (yieldd)
c              aux(i,2) =storage for last time step jump (din1)
c              aux(i,3) =storage for critical crack opening rate at ucr
(dudtcrtemp)
c              aux(i,4) =storage for Damage Variable (dam1)
c              aux(i,5) =storage for last stress for keeping nodes
together when us=0 (sign1)
c              aux(i,6) =storage for critical crack opening rate at us
(dudtstemp)
c          ek          = max. stiffness/area for time step calculation
c          ifail       =.false. not failed
c                      =.true. failed
c          dt1siz      = time step size
c          crv         =curve array - not used
c          di1 = normal displacement jump
c          di2 = mode II displacement jump
c          di3 = mode III displacement jump
c
c          dam1 = mode I damage variable
c          di23 = mode II and III combined damage variable
c          dudt = mode I crack opening rate
c
c **********
c
c     jump_u, dxdt, and fTraction are in the local coordinate system:
c     components 1 and 2 are in the plane of the cohesive surface
c     component 3 is normal to the plane
c
c     the declaration below is processed by the C preprocessor and
c     is real*4 or real*8 depending on whether LS-DYNA is single or
double
c     precision
      real L,jump_u,ck1b,ck2b,u1s,u1int,u2int,u1end,u2end,
     & u1delta,u2delta,u1ie,u2ie,dam1,dam1i,dam23i,dam23
     & ckm2,dudt,dudtcrtemp,dudtcr1,dudtstemp,dudts
     & etacs,alphabdc,syield,smax,sfrac,nubd
     & fK,fac,fpenalty
     & Kp, di1,di2,di3,di23,din1,din2,din3,sign1,one,zero

      logical ifail

      dimension params(*),fTraction(nlq,*),jump_u(nlq,*),
     &          dxdt(nlq,*),aux(nlq,*),ek(*),ifail(*),dt1siz(*),
     &          crv(101,2,*)

c     connector stiffnesses/area (3 direction normal to delam plane)
c
c     critical separation displacement to fail connector
      one=1.0
      zero=0.0
c Mode I parameters
      u1s    = params(3)  ! displacement for syield
      u1int  = params(4)  ! displacement at start of damage, ucr
      u1end  = params(5)  ! displacement at end of damage, uend
      syield = params(6) ! yield stress at u=u1s
```

```
      smax   = params(7) ! maximum stress at ucr and dudt=0
      sfrac  = params(8) ! fracture Stress
      etacs = params(9) ! viscosity parameter for smax
      nubdc  = params(10) ! viscosity parameter for syield
      Kp  = params(11) ! gain parameter for keeping nodes together when
not yielded
c Mode II and III parameters
      ckm2   = params(12) ! stiffness mode II and III
      u2int  = params(13)  ! mode II and  III critical displacement
      u2end  = params(14) ! mode II and III end displacement
c Other
      fpenalty  = params(15) ! penetration constant
c
      fK=fpenalty*smax/u1int
c intermadiate material constants
      u1delta = u1int - u1end
      u2delta = u2int - u2end
      u1ie    = u1int*u1end
      u2ie    = u2int*u2end
c Main do loop
      do i=lft,llt
         di2 = jump_u(i,1) ! mode II
         di3 = jump_u(i,2) ! mode III
         di1 = jump_u(i,3) ! normal displacement
c
         di23=sqrt(di2*di2+di3*di3) ! combined mode II and III
displacement
c Extract History Variables
         yieldd=aux(i,1) ! element yielded when equal one -  not
yeilded when qual to zero
         if(u1s.eq.zero.and.syield.eq.zero) then
            yieldd=one
            aux(i,1)=one
         endif
c
         dinl= aux(i,2) ! last time step jump
         aux(i,2)=di1 ! set for next time step
         dudtcr1=aux(i,3) !last time step dudtcrtemp
         dudts=aux(i,6) !last time step dudtcrtemp
         sign1=aux(i,5) ! last stress for keeping nodes together prior
to yield
c
c Set damage variables
c
c Mode I damage variable
         if(di1.lt.u1int) then
            dam1 = one
            aux(i,4)= one
         else if(di1.ge.u1int) then
            dam1i = (di1*u1int-u1ie)/(di1*u1delta) ! calculate
intermediate damage variable
            dam1  = max(dam1i,zero) !if negative set to zero
            dam1 = min(aux(i,4),dam1) ! store minimum positive value
            aux(i,4) = dam1 !store it
            if(dam1.le.zero) ifail(i)=.true.
 1       endif
c Mode II and III damage variable
```

```
          if(di23.gt.u2int)then
             dam23i= (di23*u2int-u2ie)/(di23*u2delta) ! calculate
intermediate damage variable mode II and III
             dam23=max(dam23i,zero) ! if negative set to zero
             if(dam23.le.zero) ifail(i)=.true.
          else
             dam23=one
          endif
c
c       CALCULATE STRESSES
c
c Rate dependent term - dudt
c
c Store cricital dudt value - Last value that gets used at u1int
          if(di1 .le. u1s) then
              if((di1-din1) .gt. zero .and. dt1siz(i) .gt. zero ) then
                dudt=((di1-din1)/dt1siz(i))
              else
                 dudt=zero
              endif
              dudtstemp= max(dudts,dudt) !new or old value
              aux(i,6) = dudtstemp !store it critical dudt
          else if(di1 .le. u1int) then
              if((di1-din1) .gt. zero .and. dt1siz(i) .gt. zero ) then
                dudt=((di1-din1)/dt1siz(i))
              else
                 dudt=zero
              endif
              dudtcrtemp= max(dudtcr1,dudt) !new or old value
              aux(i,3) = dudtcrtemp !store it critical dudt
          else
               dudtcrtemp=dudtcr1
               dudtstemp=dudts
          endif
c Assign Tractions
          if(u1s.eq.zero)then
             if(yieldd.eq.zero) then
                if(di1.le.zero) then
                   fTraction(i,3)= di1*syield/u1int+fK*di1
                else
                   fTraction(i,3)= di1*(smax/u1int)*Kp+sign1
                   if(fTraction(i,3).ge.syield) then
                      aux(i,1)=one
                      yieldd=one
                   endif
                endif
             else ! already yielded
                if(ifail(i).eq.true) then
                   fTraction(i,3)=0.0
                else if(di1.le.zero) then
                   fTraction(i,3)= di1*syield/u1int+fK*di1
                else if(di1.le.u1int) then
                   fTraction(i,3)=syield+nubdc*dudtstemp+(smax-syield +
     &          dudtcrtemp*etacs-dudtstemp*nubdc)*((di1-u1s)/(u1int-
u1s))
c                  check for negative tractions which can occur with
etacs negative
```

```
                  if(fTraction(i,3).lt.zero) then
                     fTraction(i,3)=0.0
                     ifail(i)=.true.
                  endif
               else
                  fTraction(i,3)= dam1*di1*
     &                 (smax+etacs*dudtcrtemp)/ulint
c                 check for negative tractions which can occur with
etacs negative
                  if(fTraction(i,3).lt.zero) then
                     fTraction(i,3)=0.0
                     ifail(i)=.true.
                  endif
               endif
            endif
         else                ! uls not zero
            if(ifail(i).eq.true) then
                  fTraction(i,3)=0.0
            else if(di1.le.zero) then
               fTraction(i,3)= di1*syield/uls+fK*di1
            else if(di1.le.uls) then
              fTraction(i,3)= (syield+nubdc*dudtstemp)*di1/uls
c             check for negative tractions which can occur with etacs
negative
              if(fTraction(i,3).lt.zero) then
                  fTraction(i,3)=0.0
                  ifail(i)=.true.
              endif
            else if(di1.le.ulint) then
               fTraction(i,3)=syield+nubdc*dudtstemp+(smax-syield +
     &         dudtcrtemp*etacs-dudtstemp*nubdc)*((di1-uls)/(ulint-
uls))
c              check for negative tractions which can occur with etacs
negative
               if(fTraction(i,3).lt.zero) then
                  fTraction(i,3)=0.0
                  ifail(i)=.true.
               endif
            else
               fTraction(i,3)= dam1*di1*
     &         (smax+etacs*dudtcrtemp)/ulint
               if(fTraction(i,3).lt.zero) then
                  fTraction(i,3)=0.0
                  ifail(i)=.true.
               endif
            endif
c        YIELD criteria when syield >0
            if(di1.ge.uls.and.yieldd.eq.zero.and.syield.gt.zero) then
               aux(i,1)=one     ! store yieldd in history variable
            endif
         endif
c
c       Mode 2 and Mode 3 no rate dependence
        fTraction(i,1)=ckm2*di2*dam23
        fTraction(i,2)=ckm2*di3*dam23
c
c       approximate stiffness for timestep
```

```
         if (dil .lt. 0) then
            ek(i)=fTraction(i,3)/dil+fK
            if(ek(i).gt.(smax*1000000./ulint))then
               write(13,1050)
               write(*,1050)
               ek(i)=smax*1000000./ulint
            endif
         else
            ek(i)=fTraction(i,3)/dil
            if(ek(i).gt.(smax*1000000./ulint))then
               write(13,1060)
               write(*,1060)
               ek(i)=smax*1000000./ulint
            endif
         endif
c
c FAILURE CRITERIA
        if(fTraction(i,3).gt.sfrac.and.ifail(i).eq..false.
     &  .and.sfrac.ne.zero) then
           ifail(i)=.true. ! for failure criteria
           aux(i,1)=one    ! store yield in history variable

c          diognostic info
           write(13,1010) i,fTraction(i,3)
           write(*,1010) i,fTraction(i,3)
        endif
      enddo                   !end of the i loop
c
      return
1010  format(5x,'delamination element has stress greater than sfrac'i8,
     & 1pe12.4)
1050  format(5x,'ek limit reached on penetration')
1060  format(5x,'ek limit reached')
      end
c
c
c
c
c
```

A5. Critical Portions LS-DYNA Input File for DCB Model

```
*KEYWORD
*TITLE
EPOXY CARBON FIBER
*CONTROL_PARALLEL
         4
*CONTROL_BULK_VISCOSITY
$#       q1        q2      type
  1.500000  0.060000
*CONTROL_CONTACT
$#  slsfac    rwpnal    islchk    shlthk    penopt    thkchg     orien
enmass
  0.100000     0.000         1         1         1         1         1
$#  usrstr    usrfrc     nsbcs    interm     xpene     ssthk      ecdt
tiedprj
         0         0        10         0  4.000000
$#   sfric     dfric       edc       vfc        th     th_sf    pen_sf
     0.000     0.000     0.000     0.000     0.000     0.000     0.000
$#  ignore    frceng   skiprwg    outseg   spotstp   spotdel
         0         0         0         0         0         0
*CONTROL_COUPLING
$#  unleng    untime    unforc    timidl     flipx     flipy     flipz
subcyl
  1.000000  1.000000  1.000000     0.000         0         0         0
1
*CONTROL_CPU
$#  cputim
     0.000
*CONTROL_DYNAMIC_RELAXATION
$#  nrcyck     drtol    drfctr    drterm    tssfdr    irelal     edttl
idrflg
       250  0.001000  0.9950001.0000E+30  0.900000         0  0.040000
*CONTROL_ENERGY
$#    hgen      rwen    slnten     rylen
         1         2         1         1
*CONTROL_HOURGLASS
$#     ihq        qh
         1  0.100000
*CONTROL_OUTPUT
$#   npopt    neecho    nrefup    iaccop     opifs    ipnint    ikedit
iflush
         0         3         0         0     0.000
$#   iprtf
         0
*CONTROL_SHELL
$#  wrpang     esort     irnxx    istupd    theory       bwc     miter
proj
 20.000000         0        -1         0         2         2         1
$# rotascl    intgrd    lamsht    cstyp6    tshell   nfail1    nfail4
  1.000000         0         0         1
*CONTROL_TERMINATION
$#  endtim    endcyc     dtmin    endeng    endmas
   2.00000         0     0.000     0.000     0.000
*CONTROL_TIMESTEP
```

```
$#  dtinit    tssfac      isdo    tslimt     dt2ms       lctm     erode
mslst
     0.000  0.670000         0     0.000     0.000
$#  dt2msf   dt2mslc
     0.000
*DATABASE_BINARY_D3PLOT
$#      dt      lcdt      beam     npltc
  0.02
$#   ioopt
         0
*BOUNDARY_PRESCRIBED_MOTION_SET_ID
$#     cid
heading
         1Upper Arm Velocity
$#    nsid       dof       vad      lcid        sf       vid     death
birth
         2         4         0         1  20.50000         2  100.0000
0.000
$*BOUNDARY_SPC_SET_ID
$#     cid
heading
$         1Bottom Arm Fixed
$
$ LBC set : Fixed Beam
$
$#    nsid       cid      dofx      dofy      dofz     dofrx     dofry
dofrz
$         1         0         0         1         0         0         0
0
*SET_NODE_LIST_TITLE
Fixed BEam 2
$#     sid       da1       da2       da3       da4
         1     0.000     0.000     0.000     0.000
$#    nid1      nid2      nid3      nid4      nid5      nid6      nid7
nid8
     11623     11624     11625     11626     11627     11628     11629
11630
$ nodes left out for brevity
$$$
$*CONTACT_AUTOMATIC_GENERAL_ID
$#     cid
title
$         1contact DCB
$#    ssid      msid     sstyp     mstyp    sboxid    mboxid       spr
mpr
$         0         0         0         0         0         0         0
0
$#      fs        fd        dc        vc       vdc    penchk        bt
dt
$     0.200     0.000     0.000     0.000     0.000         0
0.0001.0000E+20
$#     sfs       sfm       sst       mst      sfst      sfmt       fsf
vsf
$ 1.000000  1.000000     0.000     0.000  1.000000  1.000000  1.000000
1.000000
*PART
$# title
```

```
CZPROP
$#     pid     secid       mid     eosid      hgid      grav    adpopt
tmid
         1         1         1
*SECTION_SOLID_TITLE
Section Cohesive Zone
$#   secid    elform       aet
         1        20         1
$$
*MAT_USER_DEFINED_MATERIAL_MODELS
$$
$#     mid        ro        mt       lmc       nhv    iortho     ibulk
ig
         1 1.5400E-6        42        15         6
$#   ivect     ifail    itherm    ihyper      ieos
         1         1         0        -1
$#   ROFLG  INTFAIL       u1s     u1int     u1end    syield      smax
sfrac
     0.000  1.000000   1.00E-5 3.4400E-4   0.00700      0.02    0.0275
10.0
$#   etacs     nubdc        kp      ckm2     u2int     u2end      fpen
     0.05       0.0       1.0      80.0 3.4400E-4     0.020      0.01
*PART
$# title
PROPSHELL
$#     pid     secid       mid     eosid      hgid      grav    adpopt
tmid
         2         2         2
*SECTION_SHELL_TITLE
Section DCB Beam
$#   secid    elform      shrf       nip     propt   qr/irid     icomp
setyp
         2        16     0.830         5         1     0.000         0
1
$#      t1        t2        t3        t4      nloc     marea
  1.500000  1.500000  1.500000  1.500000         0     0.000
*MAT_ELASTIC_TITLE
Shell Composite
$#     mid        ro         e        pr        da        db  not used
         2 1.5660E-6 120.00000  0.270000     0.000     0.000
*INITIAL_VELOCITY
$
$ LBC set : initVelocity
$
$#    nsid    nsidex     boxid    irigid
         3
$#      vx        vy        vz       vxr       vyr       vzr
     0.000     0.000     0.000     0.000     0.000     0.000
*DEFINE_CURVE_TITLE
Upper Arm Velocity Curve
$
$ This is the unit load curve
$
$#    lcid      sidr       sfa       sfo      offa      offo    dattyp
         1         0     0.000     0.000     0.000     0.000
$#                a1                  o1
               0.000          1.00000000
```

```
        100.00000000          1.00000000
*DEFINE_VECTOR
$
$ LBC set : Velocity UpperBeam
$
$#      vid        xt        yt        zt        xh        yh        zh
          1     0.000     0.000     0.000  1.000000     0.000     0.000
*DEFINE_VECTOR
$#      vid        xt        yt        zt        xh        yh        zh
          2     0.000     0.000     0.000     0.000  1.000000     0.000
*DEFINE_VECTOR
$#      vid        xt        yt        zt        xh        yh        zh
          3     0.000     0.000     0.000     0.000     0.000  1.000000
*SET_NODE_LIST_TITLE
Velocity Contorl NODES
$#      sid       da1       da2       da3       da4
          2     0.000     0.000     0.000     0.000
$#     nid1      nid2      nid3      nid4      nid5      nid6      nid7
nid8
      12403     12404     12405     12406     12407     12408     12409
12410
$ nodes left out for brevity
*SET_NODE_LIST_TITLE
ALL NODES for Initial Velocity
$#      sid       da1       da2       da3       da4
          3     0.000     0.000     0.000     0.000
$#     nid1      nid2      nid3      nid4      nid5      nid6      nid7
nid8
          1         2         3         4         5         6         7
8
$ nodes left out for brevity
*DAMPING_PART_STIFFNESS
          2      0.01
*ELEMENT_SOLID
$#    eid     pid      n1      n2      n3      n4      n5      n6
n7      n8
        1       1       1     443     444       2     222     664
665     223
$ nodes left out for brevity
*ELEMENT_SHELL
$#    eid     pid      n1      n2      n3      n4
     5701       2   11493   11494   11520   11519
$ element definitions left out for brevity
*NODE
$#   nid               x               y               z      tc
rc
       1              30           -0.75               0
$ nodes left out for brevity
*END
```

A6.Crack Growth Data Extraction Code

```
/* This program takes curve file from lspost with nodes on both sides
of an interface and outputs a vs t */
/* The crack is assumed to be in the XZ plane with the crack length
growth direction in the X direction */
/* the crack length (a) is defined as: distance from edge to crack top
minus distance from edge to loading pin location (edist) */
/* A file with node xyz coordinates must be specified in following
format
   *NODE
       1     30.00000000     -0.75000000           0.000
       .
       .
       .
   endfile
*/

#include <math.h>
#include <stdio.h>
#include <stdlib.h>
#include <string.h>

#define NMAX 30000 /* Intial guess at Maximum number of NODES */
#define ELEMMAX 25000  /* Intial guess at Maximum number of ELEMENTS */
#define LINESMAX 3000000  /* MAX number of lines to scan */
#define TOL 0.0011
#define NPOPEN 1 /* Number of consecutive nodal locations where the
crack opening must be greater than umax */

int main ()
{
      int numxypairs, numnodepairs,garbage;
      int nodenumtemp;
      int i,j,k;
      int numnodes; /* total number of nodes */
      int *nodenum; /* matrix of node and element numbers (IDS)*/
      double *plottime;
      double **time, **ydisp; /*time and displacement matrices */
      double *acrack;
      double dydisp;
      double a0; /* Initial crack length from load point */
      double edist; /* Distance from End of sample to load location */
      int oldNM=NMAX;
      int newNM=NMAX;
      int *nodesearch;
      int **nodematch;

      char str[20];
      char filename[20];
      char filename2[20];

      char str2[200];
```

```
FILE *fp, *fn;
double *x,*y,*z;

double xtemp,ytemp,ztemp;
double umax; /* maximum Distance between cohesive element nodes*/

void qsortl(double *a, double *b,int n);


/*******Allocate Matrices ****************/
/* node matrices */

nodenum=malloc(NMAX*sizeof(int));

/* Read input file */
printf("Enter complete filename\n");
gets(str);
sscanf(str,"%s",filename);
fp = fopen(filename,"r");
if(fp == NULL)
{
      printf("file not available\n");
      exit (1);
}

/* Enter in umax */
printf("Enter umax(mm) \n");
gets(str);
sscanf(str,"%lf",&umax);

/* Enter in a0 */
printf("Enter ao(mm) \n");
gets(str);
sscanf(str,"%lf",&a0);

/* Enter in e */
printf("Enter edist(mm) \n");
gets(str);
sscanf(str,"%lf",&edist);

/* looking for Node no. Keyword */
for(i=0;i<=LINESMAX;i++){
      fgets(str2,sizeof(str2),fp);
      if(strncmp(str2,"Node no.",8)==0){
            break;
      }else if(strncmp(str2,"endcurve",8)==0){
            printf("endcurve found\n");
            exit(1);
      }
}


fgets(str2,sizeof(str2),fp);
sscanf(str2,"%d %5s %d",&nodenum[0],str, &numxypairs);
/* Allocate time and ydisp */
time=malloc(NMAX*sizeof(double));
```

```
        ydisp=malloc(NMAX*sizeof(double));
        for(i=0;i<NMAX;i++)
        {
              time[i]=malloc(numxypairs*sizeof(double));
              ydisp[i]=malloc(numxypairs*sizeof(double));
        }
        i=0;
        /* Reading in time disp for each node*/
        while(strpbrk(str2,"#pts=")!=NULL){
              for(j=0;j<numxypairs;j++){
                    fgets(str2,sizeof(str2),fp);
                    sscanf(str2,"%lf %lf ",&time[i][j],&ydisp[i][j]);
              }
              i++;
              /* Reallocate Matrices for time and x y data */
              if(i>=newNM-1){
                    printf("im am reallocing node matrices ");
                    oldNM=newNM;
                    newNM=(int)(oldNM*1.2);

                    nodenum = realloc(nodenum,newNM*sizeof(int *));
                    if (nodenum==NULL) {printf("not enough memory\n");
exit(1);}
                    time = realloc(time,newNM*sizeof(double *));
                    if (time==NULL) {printf("not enough memory\n");
exit(1);}
                    ydisp = realloc(ydisp,newNM*sizeof(double *));
                    if (ydisp==NULL) {printf("not enough memory\n");
exit(1);}

                    for (i=oldNM;i<newNM;i++)
                    {
                          time[i] = malloc(numxypairs*sizeof(double));
                          if (time[i]==NULL) {
                                printf("not enough memory\n"); exit(1);}
                          ydisp[i] = malloc(numxypairs*sizeof(double));
                          if (ydisp[i]==NULL) {
                                printf("not enough memory\n"); exit(1);}
                    }
              }

              fgets(str2,sizeof(str2),fp); /* get endcurve out of the way
*/
              fgets(str2,sizeof(str2),fp); /* get Node # and # points */
              sscanf(str2,"%d %6s %d",&nodenum[i],str, &garbage);
        }
        numnodes=i;
        fclose(fp);

        x=malloc(newNM*sizeof(double));
        y=malloc(newNM*sizeof(double));
        z=malloc(newNM*sizeof(double));

/****************************************************/
        /* Read node coordinate input file */
        printf("Enter node coordinate filename\n");
        gets(str);
```

```
	sscanf(str,"%s",filename2);

	fp = fopen(filename2,"r");
	if(fp == NULL)
	{
		printf("file not available\n");
		exit (1);
	}
	/* READ IN NODE COORDINATES */
	/* looking for *NODE Keyword */
	for(i=0;i<=LINESMAX;i++){
		fgets(str2,sizeof(str2),fp);
		if(strncmp(str2,"*NODE",5)==0){
			printf("*NODE found :-}\n");
			break;
		}else if(strncmp(str2,"endfile",7)==0){
			printf("endfile found\n");
			exit(1);
		}
	}
	printf("numnodes = %d\n",numnodes);
	/* Reading in X,Y,Z coordinates of nodes*/
	i=0;
	fgets(str2,sizeof(str2),fp);
	while(strncmp(str2,"endfile",7)!=0){
		sscanf(str2,"%d %lf %lf
%lf",&nodenumtemp,&xtemp,&ytemp,&ztemp);
		for(j=0;j<numnodes;j++){
			if(nodenumtemp==nodenum[j]){
				x[j]=xtemp;
				y[j]=ytemp;
				z[j]=ztemp;
				break;
			}
		}
		fgets(str2,sizeof(str2),fp);
		i++;
	}
	fclose(fp);
/*******************************************************************/

/******************************************************************/
	/* Allocate matrices for matching */
	nodesearch=malloc(numnodes*sizeof(int));

	for(i=0;i<numnodes;i++) {nodesearch[i]=0;}

	nodematch=malloc((int)(numnodes/2)*sizeof(int));
	for(i=0;i<((int)(numnodes/2));i++)
	{
		nodematch[i]=malloc(4*sizeof(int));
	}
	/* Find coincident NODES */
	k=0;
	for(i=0;i<numnodes;i++){
		if(nodesearch[i]==1){
			continue;
```

```
            }else{
                  for(j=i+1;j<numnodes;j++){
                        if((fabs((x[j]-x[i]))<=TOL)&&(fabs(z[j]-
z[i])<=TOL)){
                              nodematch[k][0]=nodenum[i];
                              nodematch[k][1]=nodenum[j];
                              nodematch[k][2]=i;
                              nodematch[k][3]=j;
                              nodesearch[j]=1;
                              k++;
                              break;
                        }
                  }
                  if(nodesearch[j]==0){
                        printf("Could not find match for node
%d\n",nodenum[i]);
                        exit(1);
                  }
            }
      }
      numnodepairs=(int)(numnodes/2);

      if(k!=numnodepairs){
            printf("Not everything matched !\n");
            exit(1);
      }
      /*allocate plottime and acrack */
      plottime=malloc(numnodepairs*sizeof(double));
      acrack=malloc(numnodepairs*sizeof(double));

      /* Calculated difference in ydisplacements */
      for(i=0;i<numnodepairs;i++){
            for(j=0;j<numxypairs;j++){
                  if((y[nodematch[i][2]]-y[nodematch[i][3]])>0.0){
                        dydisp=ydisp[nodematch[i][2]][j]-
ydisp[nodematch[i][3]][j];
                  }else{
                        dydisp=ydisp[nodematch[i][3]][j]-
ydisp[nodematch[i][2]][j];
                  }
                  if(dydisp>umax){
                        plottime[i]=time[i][j];
                        if((x[nodematch[i][2]]-edist)<a0){
                              acrack[i]=a0;
                        }else{
                              acrack[i]=x[nodematch[i][2]]-edist;

                        }
                        break;
                  }else{
                        plottime[i]=-5.0;
                  }
            }
      }
      /*Put in Time order */
      qsort1(plottime, acrack, numnodepairs);
      fn = fopen(strcat(filename,"_plot"),"w");
```

```
	fprintf(fn,"time(ms)\ta(mm)\n");
	/* Put results in _plot file */
	for(i=0;i<numnodepairs;i++){
		if(plottime[i]!=-5.0){
			fprintf(fn,"%3.9lf\t
%5.2lf\n",plottime[i],acrack[i]);
		}
	}
	fclose(fn);
	return (0);
}
```

Symbols

a	=	mode I damage term offset constant
a_{23}	=	mode I damage term offset constant
a_o	=	initial crack length of DCB specimen
b	=	mode II damage term slope constant
b_{23}	=	mode II damage term slope constant
c_s	=	characteristic wave speed $\left(\sqrt{\mu/\rho}\right)$
G_{Ic}	=	mode I critical strain energy release rate
h_1	=	arm thickness of DCB
h_2	=	arm thickness of DCB
K_{23}	=	cohesive model hardening stiffness
t	=	time
u	=	mode I crack opening displacement
u_{II}	=	mode II crack opening displacement
u_{III}	=	mode III crack opening displacement
u_{23}	=	root mean square combined mode II and II loading
$\dot{u}$	=	rate of mode I crack opening displacement
u_{cr}	=	critical mode I crack opening displacement
u_{23cr}	=	critical mode II/III crack opening displacement
$\dot{u}_{cr}$	=	historical mode I rate of crack opening displacement when $u=u_{cr}$
u_{end}	=	mode I crack opening displacement where tractions are reduced to zero
u_{23end}	=	mode II/III crack opening displacement where tractions are reduced to zero
u_s	=	yield mode I crack opening displacement
$\dot{u}_s$	=	historical mode I rate of crack opening displacement when $u=u_s$

η	=	cohesive zone viscosity for shift of $\tau_{\max}$
μ	=	shear modulus
ν	=	cohesive zone viscosity for shift of τ_y
ρ	=	density
τ	=	mode I cohesive traction
τ_{II}	=	mode II cohesive traction
τ_{III}	=	mode III cohesive traction
τ^c	=	critical cohesive traction
τ^I	=	rate-independent model constant
$\tau_{\max}$	=	maximum cohesive traction
τ_y	=	mode I yield cohesive traction
ψ	=	mode I damage variable of cohesive zone
ψ_{23}	=	damage variable of cohesive zone

Acronyms

CAI -	Composites Affordability Initiative
COD–	Crack Opening Displacement
CMOD -	Crack Mouth Opening Displacements
DCB –	Double Cantilever Beam
DFC-	Air Force's Decoupled Fuel Cells
DLL-	Design Limit Load
FEA –	Finite Element Analysis
HEI -	High Explosive Incendiary
HRAM -	Hydrodynamic Ram
JLF–	Joint Live Fire
LFT&E –	Fire Testing and Evaluation
M&S -	Modeling and Simulation